The Thesis Committee for Mohammed Ibrahim Fallatah
Certifies that this is the approved version of the following thesis:

Stratigraphy and Depositional Environments of the Late Jurassic Hanifa Formation along the Tuwaiq Escarpment, Saudi Arabia

APPROVED BY
SUPERVISING COMMITTEE:

Supervisor:

Charles Kerans

Robert G. Loucks

Rowan C. Martindale

Stratigraphy and Depositional Environments of the Late Jurassic Hanifa Formation along the Tuwaiq Escarpment, Saudi Arabia

by

Mohammed Ibrahim Fallatah, B.S.

Thesis

Presented to the Faculty of the Graduate School of

The University of Texas at Austin

in Partial Fulfillment

of the Requirements

for the Degree of

Master of Science in Geological Sciences

The University of Texas at Austin

May, 2017

Dedication

To my beloved wife, Bayan, for the unprecedented support through her love and sacrifices.

To my daughter, Lateen, for being the joy and colors of my life that reminded me to keep pushing on.

To my precious parents, for their prayers, encouragement, and for raising the man I am today.

To my big family and friends, for their encouragement and best wishes.

Acknowledgements

My gratitude would never be extended enough to recognize the support and efforts poured into my project. Great thanks go to Saudi Aramco for the graduate sponsorship. To the Reservoir Characterization Department's management, Aus Al-Tawil, Abdullah Al-Shamsi, Jamil Al-Hajhog, and Abdulaziz Al-Gaoud, for their unparalleled support throughout the course of my studies. Many thanks go to Fawwaz Al-Khaldi his great mentorship and help. To Majed Al-Ghamdi for assisting with fieldwork. To Abdullah Al-Mojel for graciously sharing his data. To my senior stratigraphers at Saudi Aramco, Mahmoud Al-Nazgah, Yousef Mousa, and Khalaf Al-Temimi, for their inputs and constructive discussions. Thanks to Aramco's core facility personnel for their support. To Dr. Stephen Hasiotis for his help in ichnofossils identification. To my committee, Bob Loucks and Rowan Martindale, for their valuable comments to improve my thesis. Last but not least, a great deal of thanks and appreciation is due to Charles Kerans for his teaching, guidance, and words of encouragement that pushed me to produce a fine project.

Abstract

Stratigraphy and Depositional Environments of the Late Jurassic Hanifa Formation along the Tuwaiq Escarpment, Saudi Arabia

Mohammed Ibrahim Fallatah, M.S.Geo.Sci.

The University of Texas at Austin, 2017

Supervisor: Charles Kerans

A sequence stratigraphic framework of the Late Jurassic (Oxfordian) Hanifa Formation at its exposure in Central Arabia is presented for the first time. This study offers the first high-resolution stratigraphic framework of the Hanifa along the Tuwaiq Escarpment by measuring 15 sections (~770 m total thickness) over an oblique-to-dip distance of 260 km and collecting 295 samples for petrographic analysis. On the basis of these data, the Hanifa Formation can be subdivided into eight facies; 1) tabular cross-bedded quartz-peloidal-skeletal grainstone, 2) cross-bedded skeletal-peloidal grainstone, 3) bioturbated foraminiferal wackestone/mud-dominated packstone, 4) oncolitic rudstone, 5) stromatoporoid-coral biostrome/bioherm, 6) peloidal/composite-grain grain-dominated packstone/grainstone, 7) bioturbated spiculitic wackestone/mud-dominated packstone, and 8) thinly-bedded argillaceous mudstone/wackestone. The vertical and lateral distributions of these facies along the exposure define their sequence setting using the principals of sequence stratigraphy. By recognizing erosional surfaces, facies offset, and changes in facies proportions, five composite sequences, with an average duration of 1.1 my, are interpreted for the Hanifa Formation. The correlation of the sequences across the study area shows that only four sequences are preserved in the north where shallow-water deposits

are well-developed. Facies trends within these sequences are further illustrated in a depositional model, which depicts the presence of an offshore structurally controlled skeletal-peloidal shoal body described here for the first time at the Hanifa exposure in the Hozwa area. A ramp depositional model is proposed having normal open-marine conditions and characterized by a high-energy inner-ramp shoreline, which is documented herein for the first time. This work provides a predictive framework and outcrop analog for applications in hydrocarbon exploration and development. Furthermore, a basinal setting predicted to the south of the study area is a potential site for unconventional plays.

Table of Contents

List of Tables ix

List of Figures x

INTRODUCTION 1

GEOLOGICAL SETTING AND STRATIGRAPHY 3

DATA AND METHODS 6

SEDIMENTOLOGY OF THE HANIFA FORMATION 9

- Tabular cross-bedded quartz-peloidal-skeletal grainstone 12
- Cross-bedded skeletal-peloidal grainstone 14
- Bioturbated foraminiferal wackestone/mud-dominated packstone (MDP) 16
- Oncolitic rudstone 18
- Stromatoporoid-coral biostrome/bioherm 20
- Peloidal/composite-grain grain-dominated packstone (GDP)/grainstone 22
- Bioturbated echinoderm-brachiopod wackestone/mud-dominated packstone 26
- Bioturbated spiculitic wackestone/mud-dominated packstone 27
- Thinly-bedded argillaceous mudstone/wackestone 29

SEQUENCE STRATIGRAPHIC FRAMEWORK OF THE HANIFA FORMATION 32

DEPOSITIONAL MODEL OF THE HANIFA FORMATION 43

DISCUSSION 45

- Study findings from the perspective of previous works 45
- Comparison with similar Jurassic systems 49
- Implications for hydrocarbon exploration and development 50

CONCLUSIONS.....52

APPENDIX.....54

REFERENCES 65

List of Tables

Table 1: List of the Hanifa Formation measured sections along the Tuwaiq Escarpment in Central Arabia. 7

Table 2: Summary of the Hanifa Formation depositional facies arranged from proximal to distal settings. 10

List of Figures

Fig. 1. Paleogeographic maps for the Arabian Plate during the Late Jurassic.....4

Fig. 2. The Late Jurassic stratigraphic column of Saudi Arabia. 5

Fig. 3. Google Earth images for the localities studied. 8

Fig. 4. Jabal Al-Abakkayn measured section showing the vertical distribution of the Hanifa and Jubaila facies 11

Fig. 5. Tabular cross-bedded quartz-peloidal-skeletal grainstone facies 13

Fig. 6. Cross-bedded skeletal-peloidal grainstone facies 16

Fig. 7. Bioturbated foraminiferal wackestone/mud-dominated packstone facies. .17

Fig. 8. Oncolitic rudstone facies. 19

Fig. 9. Stromatoporoid-coral biostrome/bioherm facies 22

Fig. 10. Peloidal/composite-grain grain-dominated packstone/grainstone facies (tempestites). 25

Fig. 11. Bioturbated echinoderm-brachiopod wackestone/mud-dominated packstone facies 27

Fig. 12. Bioturbated spiculitic wackestone/mud-dominated packstone facies 28

Fig. 13. Thinly-bedded argillaceous mudstone/wackestone facies.....31

Fig. 14. Cross-section showing the sequence stratigraphic framework of the Hanifa Formation datumed on the Hanifa-Jubaila contact. 33

Fig. 15. Individual composite sequences of the Hanifa Formation showing depositional variations spatially through time. 35

Fig. 16. Detailed stratigraphic framework of the Hanifa composite sequences 4 and 5 in the Hozwa area.....38

Fig. 17. Unconformity surface recognized in the Hozwa area. 40

Fig. 18. Correlation between Jabal Al-Abakkayn measured sections 42
Fig. 19. Idealized depositional model for the Hanifa Formation.....44
Fig. 20. The Hanifa Formation exposure in Raghbah and Wadi Dirab. 46
Fig. 21. The contact between the Hanifa and Jubaila Formations recognized in the field 47
Fig. 22. The interpreted paleoshoreline during the HST of Hanifa 48

INTRODUCTION

The Hanifa Formation is an important Jurassic unit in Saudi Arabia that has economic conventional hydrocarbon accumulations in many oilfields, as well as unconventional potential as a source rock in basinal areas of the Arabian Platform (Alsharhan and Magara, 1994). Due to the economic importance and potential of the Hanifa Formation, a detailed understanding of the sedimentology and stratigraphy of this unit is needed. Examining the surface geology of the Hanifa Formation is the first step towards establishing that understanding in order to help constructing reservoir models that adequately describe the Hanifa Reservoir architecture and flow units and to explore for new targets in the subsurface. Outcrop-based work set the objectives for recognizing the Hanifa depositional facies and their environments at a regional scale that can provide analogs for subsurface studies. The rationale behind this investigation is that the outcrop belt of the Hanifa Formation is relatively close (~150 km) to large commercial hydrocarbon fields in Saudi Arabia, which allows correlation between surface geology with that of the subsurface.

The exposures of sedimentary strata, including the Hanifa Formation, along the Tuwaiq Mountains have received considerable attention since these strata were first described by Bramkamp and Steineke (1952), Powers et al. (1966), and Powers (1968). Much of this work was done during the regional mapping of the Tuwaiq Mountains by Vaslet et al. (1983, 1991) and Manivit et al. (1985). These studies were conducted to provide lithostratigraphic, biostratigraphic, and structural descriptions for the exposure belt. Other sedimentological investigations on the Hanifa Formation exposure include the work of Okla (1983, 1986) and Moshrif (1984). Also, detailed paleontological studies on the Hanifa were presented in El-Asa'ad (1991), Hughes (2004, 2009), Hughes et al. (2008), and El-Sorogy and Al-Sahtany (2015). The common denominator between these studies is their generic descriptions of the Hanifa exposure, and to date, there has been no detailed documentation of the sedimentology of the Hanifa facies. Although Okla (1983, 1986) documented the sedimentology of the Hanifa, the resolution of their descriptions was low

to be used for constructing a stratigraphic framework. In contrast, Hughes et al. (2008) and Hughes (2009) acquired high-resolution paleontological data through petrographic analysis of outcrop samples, however, these were not integrated with sedimentological analysis on the Hanifa exposures in a stratigraphic context.

Previous studies on the Hanifa exposures also sought to provide paleoenvironmental interpretations and propose depositional models for the formation. Nevertheless, because the Hanifa facies descriptions were much generalized, the presented interpretations are oversimplified. In his work on the Hanifa outcrops, Okla (1983) described the depositional setting of the Hanifa facies as ranging from deep low-energy conditions to shallower water, higher energy oxygenated conditions. Contrarily, Hughes et al. (2008) proposed a depositional model covering the Hanifa Formation over the entire Arabian Platform, where a lagoonal setting was generally prevalent where the exposure belt is. A similar depositional setting was also proposed by Moshrif (1984). However, Hughes et al. (2008) based their depositional model on paleontological data without incorporating detailed sedimentology of the Hanifa facies. This lack of integrated data led Hughes et al. (2008) to have a limited view of the Hanifa depositional environments.

This present study, based on facies associations from sedimentological and petrographic descriptions observed from outcrop data, presents a detailed interpretation of the Hanifa outcrop area. These data are used to construct a high-resolution sequence stratigraphic framework and a robust depositional model for the Hanifa Formation. The results present a refined understanding of the Hanifa sedimentology and provide a stratigraphic framework that was not done by earlier workers. In addition, this study provides an outcrop analog for comparison and correlation with subsurface data.

GEOLOGICAL SETTING AND STRATIGRAPHY

The Hanifa Formation is exposed in Central Arabia along the Tuwaiq Mountains Escarpment (Fig. 1). The exposure belt trends north-south for ~700 km, bordering the eastern margin of the Precambrian Arabian Shield (Okla, 1983). The Tuwaiq Escarpment hosts Phanerozoic sedimentary rocks that form west-facing cliffs, in which the strata have a 1^{o} northeast dip (Vaslet et al., 1983, 1991; Manivit et al., 1985). These rocks were deposited in a relatively stable passive margin that extended from the eastern edge of the Arabian Shield in the west to as far east as the Zagros Mountains in Iran (Alsharhan and Magara, 1994; Ziegler, 2001; Lindsay et al., 2006).

During the Late Jurassic, most of the Arabian Shelf was located south of the equator (Figs. 1A and 1B). A shallow sea covered the shelf as an extension of the western Tethys Ocean (Manivit et al., 1985; Hughes et al., 2008), where the area was characterized by a humid climate (Markello et al., 2007). During the time of Hanifa deposition, a shallow-marine setting was prevalent, resulting in the deposition of carbonate sediments across the Arabian Shelf.

Stratigraphically, the Hanifa Formation is underlain by the Tuwaiq Mountain Limestone and overlain by the Jubaila Formation (Fig. 2). The contact with the Tuwaiq Mountain Limestone is a paraconformity surface whereas the upper contact with the Jubaila Formation is a disconformity surface (Hughes et al., 2008). The top of the coral-stromatoporoid reefs of the Tuwaiq Mountain Limestone defines the basal contact of the Hanifa (Hughes, 2009), whereas the upper contact is defined by a facies offset that separates grainstones of the upper Hanifa from wackestones of the Jubaila (Manivit et al., 1985). The Hanifa Formation is about 90 – 140 m thick along the exposure, which spanned a maximum depositional period of 5.5 million years (Hughes et al., 2008). The Hanifa Formation was divided by Vaslet et al. (1983) into two members, the lower Hawtah Member is dominated by muddy argillaceous limestone with multiple grainstone and coral-bearing layers. The overlying member, Ulayyah, is dominated by grainstone beds and stromatoporoid and coral-bearing biostromes and bioherms (Manivit et al., 1985; Vaslet et

al., 1991, 1983). In the subsurface, the Hanifa Reservoir is equivalent to the upper part of the Ulayyah Member (Hughes, 2004).

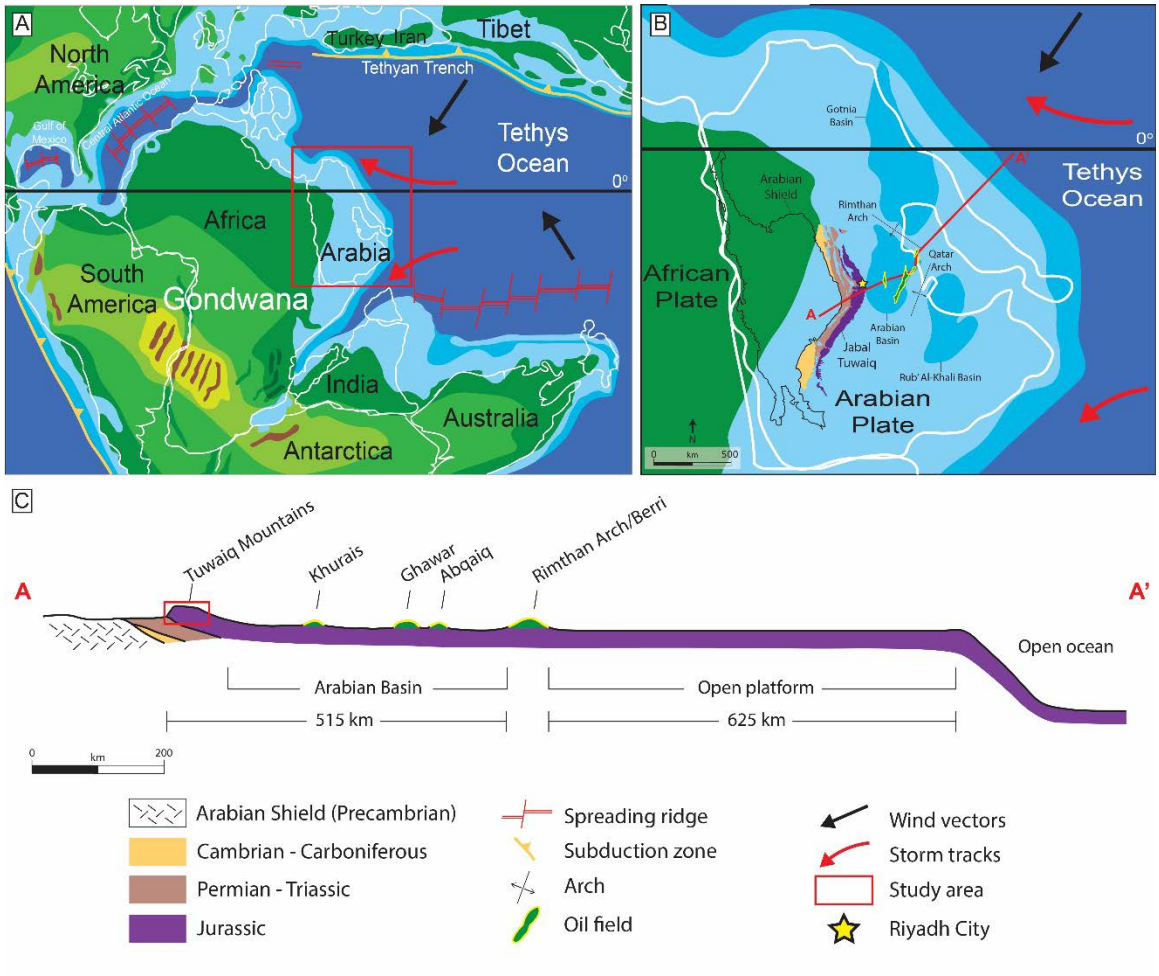

Fig. 1. Paleogeographic maps for the Arabian Plate during the Late Jurassic, 152 Ma (modified after Scotese, 2002). (**A**) The Arabian Plate was at an equatorial position in the Late Jurassic facing the western Tethys Ocean. The prevailing winds affecting the shallow-water Arabian Platform were northeastern (Markello et al., 2007). (**B**) A close-up view of the Arabian Plate during Late Jurassic showing a shallow-marine platform with three intrashelf basins (Ziegler, 2001). The Jurassic sedimentary units are exposed along the Tuwaiq Mountains Belt (Jabal Tuwaiq) that borders the Arabian Shield (Fischer et al., 2001). (**C**) A schematic cross-section of the Arabian Platform showing the location of the study area (red box) relative to the broad platform.

The Hanifa Formation is assigned to Oxfordian – Early Kimmeridgian (Fig. 2). Ammonite fauna *Euaspidoceras perarmatum* encountered in the upper part of the Hawtah Member indicates a Middle Oxfordian age (Vaslet et al., 1983; Manivit et al., 1985). This age assignment is also supported by brachiopods species *Somalirhynchia africana*, *Somalithyris bihendulensis*, and *Rhynchonella hadramautensis*, which suggest Early to Middle Oxfordian age (Vaslet et al., 1991). The Ulayyah Member is assigned to the Late Oxfordian – Early Kimmeridgian according to the recognized echinoid species *Pygurus smelthei* and *Polycyphus parvituberculatus* (Manivit et al., 1985).

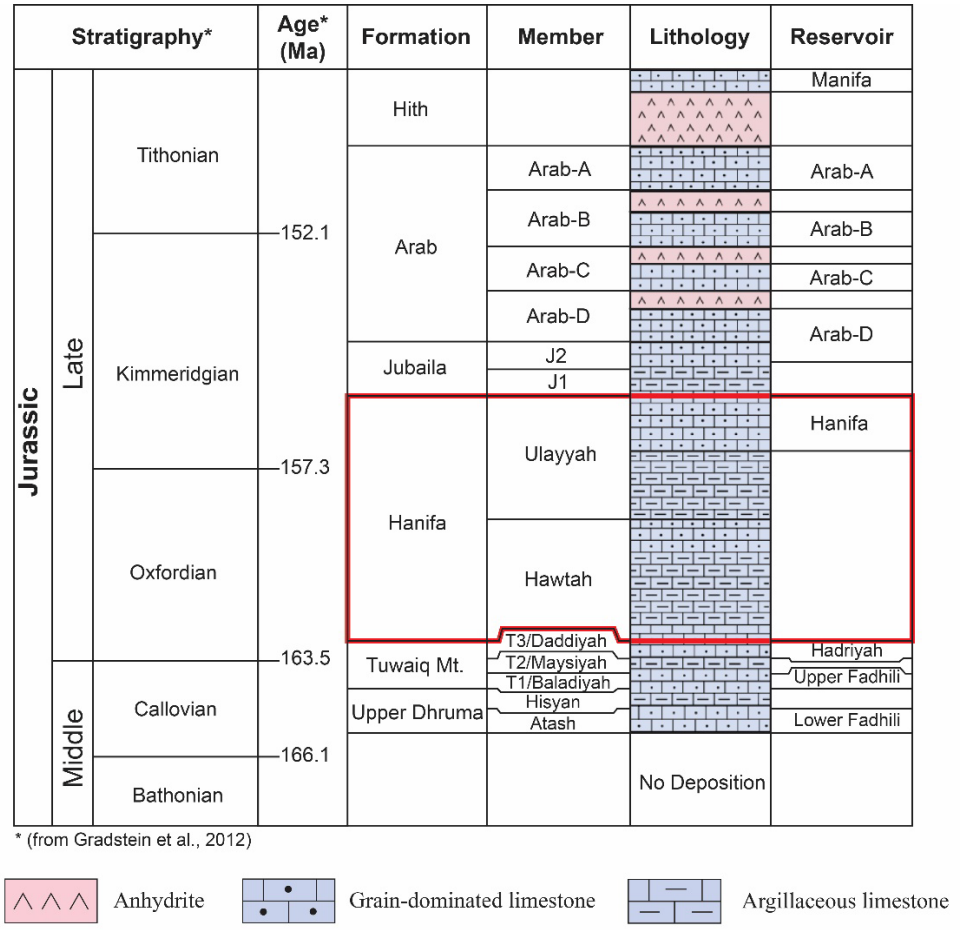

Fig. 2. The Late Jurassic stratigraphic column of Saudi Arabia. The Hanifa Formation has a mixed lithology of argillaceous limestone and pure carbonate (modified after Hughes, 2004).

DATA AND METHODS

The dataset for this study includes 15 measured sections of the Hanifa Formation along the Tuwaiq Escarpment, in addition to three measured sections provided by Abdullah Al-Mojel (Table 1; Fig. 3; Appendix). Seven of the measured sections describe the complete Hanifa sequence and 11 sections cover only parts of the unit because of exposure limitation. Sections, where permitted, were started from the distinctive top of the underlying Tuwaiq Mountain Limestone. Otherwise, the measured sections continued into the lower part of the Jubalia Formation since the upper contact of the Hanifa is not well constrained everywhere. At each section, facies were described based on color, sedimentary structures, ichnofacies, grain types, bedding styles, and rock textures. For textural description, Dunham's (1962) classification was primarily used and the modified version of this classification by Embry & Klovan (1971) was utilized where it was appropriate. The terminology described in Campbell (1967) was used to describe bedding style, while the degree of bioturbation was described based on Taylor and Goldring's (1993) classification. The dataset also includes 295 samples that were collected from the field and cut into thin sections impregnated with blue-dyed epoxy for petrographic analysis to recognize grain types and microfacies. Primarily, the biostratigraphic studies on the Jurassic of Hughes (2004) and Hughes et al. (2008) were referred to extensively for recognizing foraminiferal types and other fauna of the Jurassic formations.

A regional cross-section of the Hanifa Formation along the Tuwaiq Mountains Escarpment over a distance of 260 km was constructed after integrating 11 measured sections (Fig. 3). The top of the Hanifa Formation was selected as a datum for the cross-section. Also, two additional cross-sections incorporating seven and three measured sections were generated for transects of less than eight kilometers and 1.5 kilometers, respectively, in order to define a rapid lateral facies change and the contact character between the Hanifa and Jubaila Formations. Correlations between the sections are based on the interpreted composite sequences defined using sequence stratigraphic concepts described in Kerans and Tinker (1997). Primarily, facies proportion and sharp

Section Name	Start of Section		End of Section		Thickness (m)	Number of Samples
	Latitude	Longitude	Latitude	Longitude		
Raghbah	25°13'6.00"N	45°57'25.00"E	25°12'52.69"N	45°58'4.68"E	86.75	19
Huraymila	25° 9'21.00"N	46° 6'38.00"E	25° 9'20.64"N	46° 6'41.12"E	36.00	6
Sadous	25° 1'5.00"N	46°10'56.00"E	25° 1'8.00"N	46°11'13.00"E	76.80	——
Hozwa 1	25° 0'57.00"N	46°16'8.00"E	25° 0'57.38"N	46°16'8.27"E	11.25	8
Hozwa 2	25° 0'15.10"N	46°15'27.75"E	25° 0'14.86"N	46°15'29.42"E	24.00	11
Hozwa 3	24°59'28.98"N	46°14'18.20"E	24°59'28.00"N	46°14'17.81"E	13.00	1
Hozwa 4	25° 0'9.41"N	46°15'24.15"E	25° 0'8.43"N	46°15'26.27"E	26.25	——
Hozwa 5	25° 0'11.00"N	46°15'27.00"E	25° 0'10.00"N	46°15'28.00"E	16.00	1
Hozwa 6	24°59'28.00"N	46°14'14.00"E	N/A		22.00	3
Jabal Al-Abakkayn 1	24°57'37.00"N	46°11'33.00"E	24°57'59.00"N	46°13'27.00"E	114.00	23
Jabal Al-Abakkayn 2	24°57'38.00"N	46°14' 9.00"E	N/A		23.00	3
Jabal Al-Abakkayn 3	24°57'27.00"N	46°14'18.00"E	N/A		25.65	5
Wadi Laban*	24°38'47.36"N	46°35'55.79"E	N/A		124.00	——
Wadi Dirab	24°26'31.96"N	46°34'57.06"E	24°26'49.42"N	46°35'2.29"E	122.00	121
Wadi Al-Ain 1	24° 6'51.19"N	46°45'2.20"E	24° 6'48.29"N	46°45'5.18"E	47.50	35
Wadi Al-Ain 6	24° 3'27.00"N	46°38'34.00"E	24° 2'59.00"N	46°38'14.00"E	123.25	5
Hawtah*	23°33'27.94"N	46°43'19.72"E	N/A		123.25	——
Wadi Birk*	23°15'20.53"N	46°43'52.52"E	N/A		156.00	——

* Measured outcrop sections provided by Abdullah Al-Mojel

Table 1: List of the Hanifa Formation measured sections along the Tuwaiq Escarpment in Central Arabia.

facies offset in each vertical profile helped in identifying the composite sequences. Conversely, most of the individual high-frequency cycles display asymmetrical, shallowing-upward stacking patterns. This was recognized based on one or more of the following trends: (1) an upward decrease in bioturbation intensity (Knaust, 1998), (2) changes in faunal assemblage, (3) an upward increase in sorting and grain size, and/or (4) an upward development of bedforms.

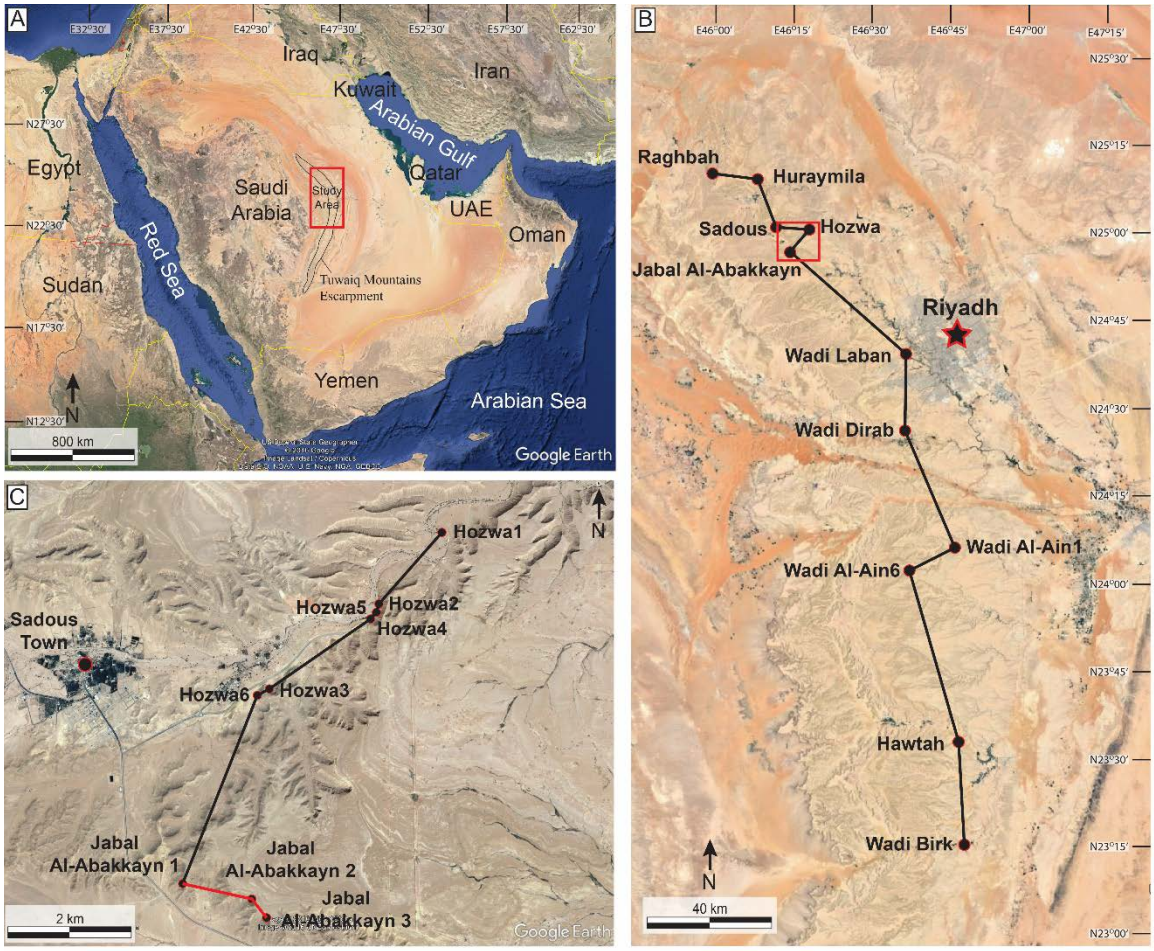

Fig. 3. Google Earth images for the localities studied. (**A**) The study area is located in Central Arabia along the Tuwaiq Mountains Escarpment in Saudi Arabia. (**B**) The relative locations of the 11 measured sections of the Hanifa Formation are highlighted, which were used to create a N-S regional cross-section [**Fig. 13**]. The red box marks the area for the second cross-section created. (**C**) Seven measured sections were used to create a cross-section [black line] over a relatively short distance to demonstrate rapid lateral facies changes illustrated in **Fig. 14**. Another cross-section [red line] incorporating three measured sections was created to illustrate the character of the contact between the Hanifa and Jubaila Formations [**Fig. 18**].

SEDIMENTOLOGY OF THE HANIFA FORMATION

Eight facies have been determined from the described sections that characterize the entire depositional settings of the Hanifa Formation in the study area and one facies from the Jubaila Formation is also identified (Table 2). The facies are composed of a diverse spectrum of sedimentary structures, ichnofabrics, and faunal assemblages (Fig. 4). This spectrum of features reflects different depositional environments. Each facies is described below and an interpretation of the depositional environment is presented.

Facies	Bedding	Fabric	Sedimentary Structures	Constituent Grains	Ichnofossils	Depositional Environment
Tabular cross-bedded quartz-peloidal-skeletal grainstone	Thin - thick (5 - 50 cm)	Moderately - well-sorted, very fine - medium (60 - 490 µm)	Low-angle cross-bedding (2° – 17°)	Echinoids (75 - 625 µm), brachiopods (310 - 490 µm), peloids (75 - 300 µm), foraminifera (105 - 250 µm), angular - subangular quartz (60 - 195 µm)		High-energy (Upper shoreface)
Cross-bedded skeletal-peloidal grainstone	Medium - thick (10 - 100 cm)	Moderately - well-sorted, very fine - medium (105 - 500 µm)	Low-angle cross-bedding (5° – 12°)	Peloids (105 - 490 µm), echinoids (120 - 1040 µm), foraminifera (210 - 1040 µm), brachiopods (220 - 1040 µm), ooids (150 - 270 µm), mollusks (500 - 4000 µm), *Clypeina* (165 - 415 µm)		High-energy [shoal] (Upper shoreface)
Biotrubated foraminiferal wackestone/mud-dominated packstone	Not preserved	Poorly-sorted, very fine - coarse (25 - 540 µm)		Foraminifera (*Kurnubia palastiniensis, Nautiloculina oolithica, Alveosepta jaccardi* ; 100 - 540 µm), brachiopods (80 - 2000 µm), echinoids (80 - 510 µm), quartz (25 - 135 µm)	*Planolites, Thalassinoides;* Bioturbation index (BI; Taylor and Goldring, 1993) – 5 - 6	Low-energy (Proximal lower shoreface)
Oncolitic rudstone	Medium - thick (45 - 95 cm)	Poorly-sorted, fine - granule (0.2 - 10 mm)	Massive	Type 3 *Bacinella – Lithocodium* oncoids (1.3 - 6.6 mm), foraminifera, brachiopods, echinoids, intraclasts, corals, stromatoporoids		Low-energy (Proximal lower shoreface)
Stromatoporoid-coral biostrome/bioherm	Medium - very thick (0.15 - 11 m)	Very poorly-sorted, fine - cobble	Massive	Corals (*Latiastrea greppini, Synastrea delemontana, Coenastraea abakkaynata, Microphyllia sommeringi,* and *Koilomorpha hanifaensis*), stromatoporoids, sponge spicules		Bioherms: high-energy (proximal lower shoreface) Biostromes: low-energy (distal lower shoreface)
Peloidal/composite-grain grain-dominated packstone /grainstone	Thin - thick (5 - 90 cm)	Poorly to very well-sorted, very fine - very coarse (60 - 2000 µm)	Hummocky cross-stratification, low-angle lamination (4° - 8°), mega-ripples	Peloids (60 - 155 µm), foraminifera (60 - 940 µm), composite grains (410 - 1250 µm), brachiopods (170 - 940 µm), echinoids (115 - 2000 µm), subangular - subrounded quartz (40 - 190 µm; 20 - 60%)	*Planolites, Rhizocorallium* , *Thalassinoides*; BI = 2	High-energy [tempestites] (Lower shoreface)
Bioturbated echinoderm-brachiopod wackestone/ mud-dominated packstone*	Not preserved	Poorly-sorted, very fine - granule (40 - 4280 µm)		Brachiopods (125 - 4280 µm), echinoids (80 - 315 µm), mollusks (135 - 1660 µm), foraminifera (200 - 560 µm), sponge spicules (50 - 270 µm), subangular - subrounded quartz (40 - 175 µm)	*Planolites, Thalassinoides, Rhizocorallium* ; BI = 5 - 6	Low-energy (Lower shoreface)
Bioturbated spiculite wackestone/mud-dominated packstone	Nodular	Poorly-sorted, very fine - granule (55 - 6000 µm)		Sponge spicules (55 - 1470 µm), foraminifera (80 - 375 µm), echinoids (70 - 400 µm), mollusks (190 - 1070 µm), brachiopods (350 - 6000 µm)	Planolites, and Chondrites; BI = 4 - 5	Low-energy (Distal lower shoreface)
Thinly-bedded argillaceous mudstone/wackestone	Thin - medium (5 - 20 cm)	Poorly-sorted, very fine - medium (55 - 400 µm)		Sponge spicules (55 - 400 µm)		Low-energy, low oxygen levels (Offshore)

* Facies in Jubaila Formation

Table 2: Summary of the Hanifa Formation depositional facies arranged from proximal to distal settings.

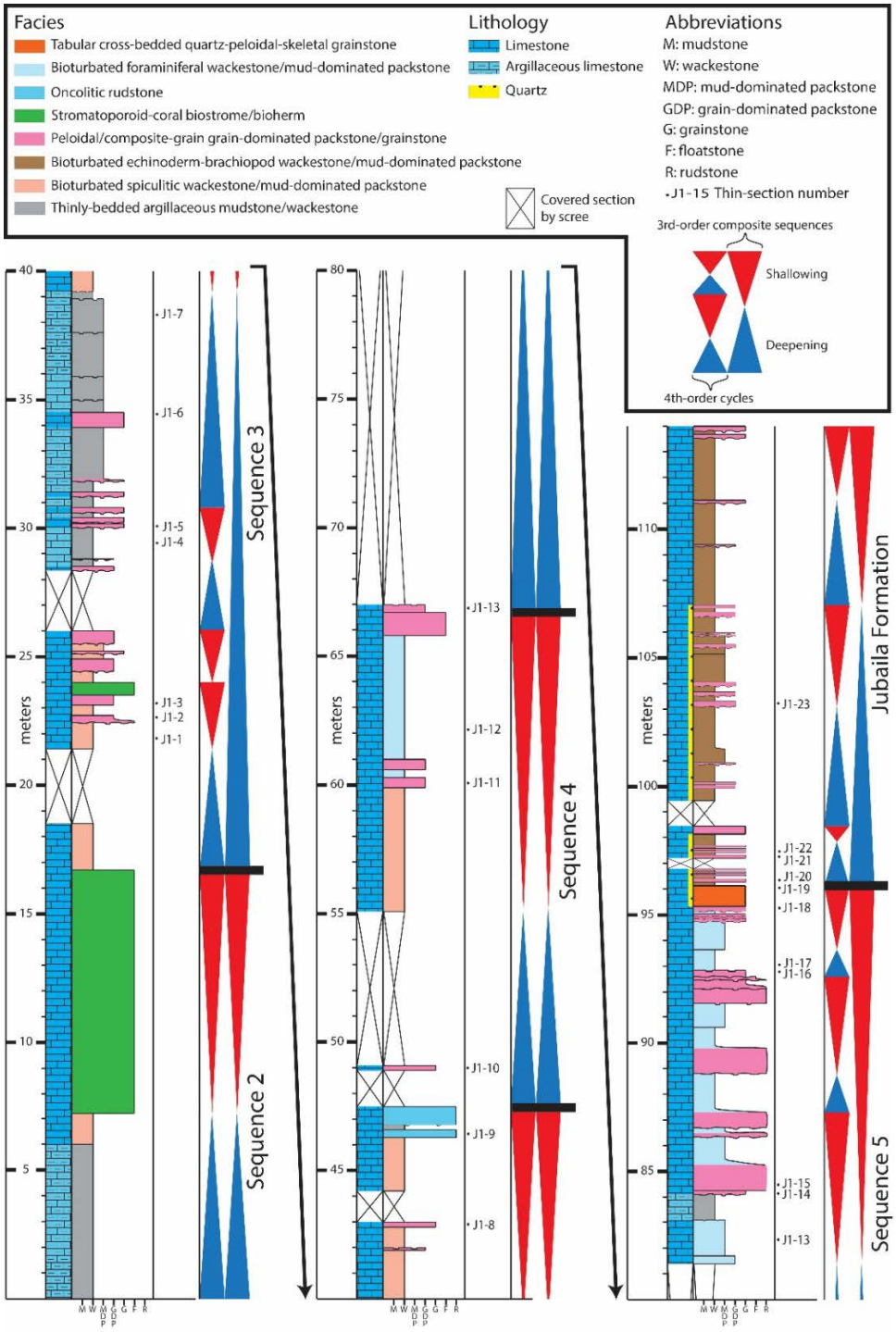

Fig. 4. Jabal Al-Abakkayn measured section showing the vertical distribution of the Hanifa and Jubaila facies starting from the contact with the underlying Tuwaiq Mountain Limestone.

TABULAR CROSS-BEDDED QUARTZ-PELOIDAL-SKELETAL GRAINSTONE

The quartz-skeletal-peloidal grainstone facies is characterized by well-defined 5 – 50 cm thick brown beds. These beds are characterized by 4º – 17º ENE-dipping foresets of cross-beds (Fig. 5A). Another distinctive feature is the presence of chert nodules at discrete intervals, which are commonly observed forming at bedding contacts. Compositionally, the grainstones are moderately to well-sorted, fine to medium grains of echinoderms, brachiopods, peloids, and foraminifera. Occasionally angular to subangular quartz grains exist and make up 10 – 20% of the constituent grains (Figs. 5C, 5D, and 5E). Also, pebble-size coral fragments are found locally.

An upper shoreface environment is interpreted for the tabular cross-bedded quartz-skeletal-peloidal grainstone facies. This is inferred from the well-sorted fabric, which indicates continuous reworking by high-energy waves (Nichols, 2009). The facies lacks the micritic matrix observed in the underlying bioturbated foraminiferal facies, which supports a higher energy setting. In addition, development of cross-bedding above fair-weather wave base is one of the key features for the upper shoreface environment (Clifton, 2006).

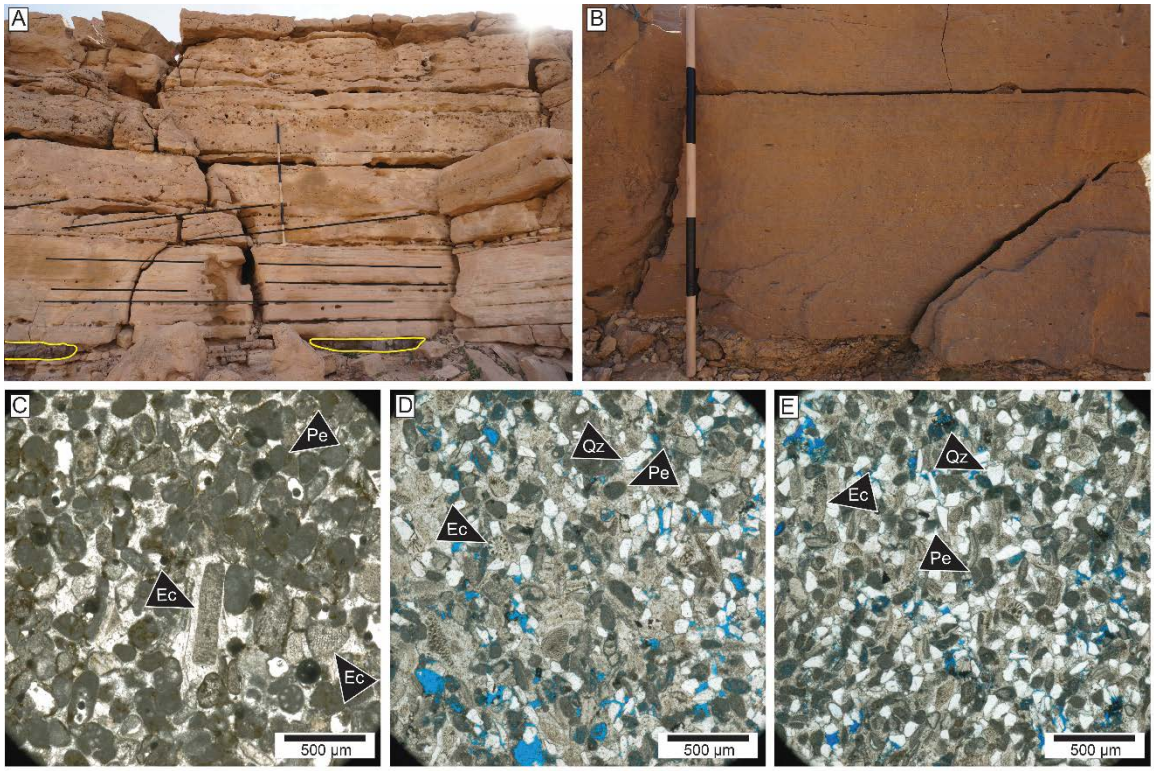

Fig. 5. Tabular cross-bedded quartz-peloidal-skeletal grainstone facies. (**A**) The general expression of the sandy peloidal-skeletal grainstone facies at the Raghbah section showing planar to low-angle stratification with chert nodules [yellow polygons] at the base [staff = 120 cm]. (**B**) At Jabal Al-Abakkayn section, the facies thins down to ~1 m and it has low-angle laminations [staff intervals = 20 cm]. (**C**) Photomicrograph under plane-polarized light from Raghbah showing a cemented grainstone dominated by peloids [Pe] and echinoderm fragments [Ec]. (**D**) Photomicrograph under plane-polarized light also from Raghbah displaying echinoderm fragments [Ec], peloids [Pe], and quartz grains [Qz] in a grainstone texture. (**E**) A similar grain association is also observed in the photomicrograph under plane-polarized light from Jabal Al-Abakkayn.

CROSS-BEDDED SKELETAL-PELOIDAL GRAINSTONE

The most prominent features of the skeletal-peloidal grainstone facies are the large cross-bed sets (Figs. 6A and 6B). Individual beds are medium to thickly bedded (10 – 100 cm), whereas a bed set can be as thick as 5 m. Low angles of 5^{o} – 12^{o} characterize the foresets of the cross-beds that dip to the northeast whereas bedding surfaces can dip as much as 5^{o} to the southwest. Compositionally, well-sorted and very fine to medium-size peloids are the main constituents (Figs. 6C, 6D, and 6E). Other grains associated with the peloidal grainstone facies include echinoderms, foraminifera, and brachiopods. Moreover, ooids and the dasycladacean green algae *Clypeina sulcata* are sparsely present.

The well-developed cross-bedding indicates an upper shoreface depositional setting above fair-weather wave base (FWWB) (Clifton, 2006). This interpretation is supported by the grainy and relatively well-sorted fabric. Also, this facies is found overlying the bioturbated foraminiferal facies.

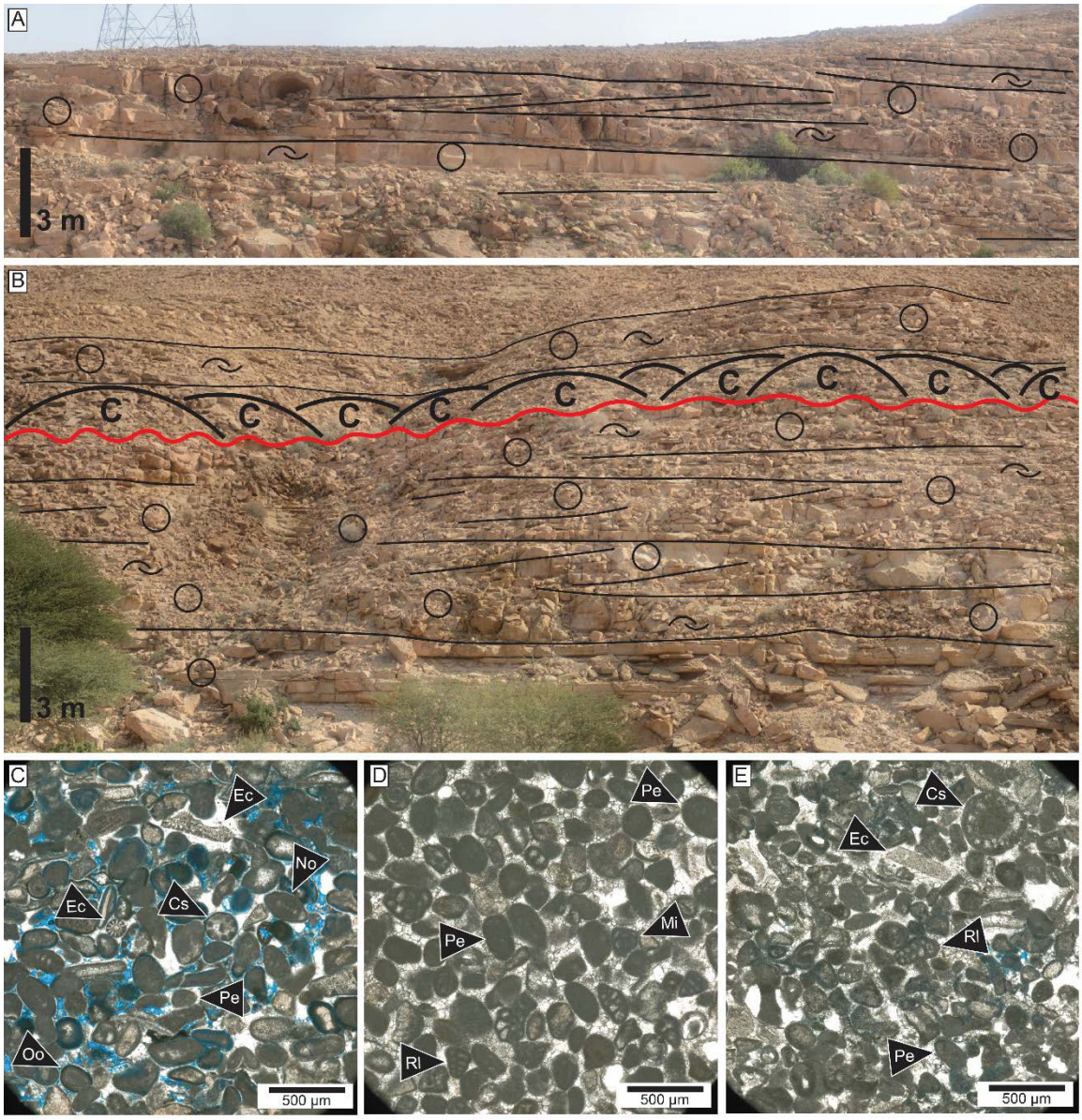
A
3 m
B
C
3 m
C
Ec
No
Ec
Cs
Pe
Oo
500 µm
D
Pe
Mi
Pe
Rl
500 µm
E
Cs
Ec
Rl
Pe
500 µm

Fig. 6

Fig. 6. Cross-bedded skeletal-peloidal grainstone facies. (**A**) This facies was only encountered near Hozwa Town where large bedforms of cross-bedding are well-exposed [circles = peloids; shell symbols = skeletal grains]. (**B**) The cross-bedded peloidal grainstones are ~ 12m thick where the top is an erosional surface [red line] and is overlain by coral buildups [circles = peloids; shell symbols = skeletal grains]. (**C**) Photomicrograph under plane-polarized light showing a grainstone dominated by echinoderms [Ec], foraminifera species *Nautiloculina oolithica* [No], and peloids [Pe]. Other sparse grains include ooids [Oo] and dasycladacean algae *Clypiena sulcata* [Cs]. Intergranular porosity is developed after cement dissolution. (**D**) Photomicrograph under plane-polarized light showing a cemented well-sorted fabric of peloids [Pe], foraminifera species *Redmondoides lugeoni* [Rl], and miliolids [Mi]. (**E**) Photomicrograph under plane-polarized light displaying moderately- to well-sorted fabric of echinoderms [Ec], peloids [Pe], *Clypiena sulcata* [Cs], and foraminifera species *Redmondoides lugeoni* [Rl].

BIOTURBATED FORAMINIFERAL WACKESTONE/MUD-DOMINATED PACKSTONE (MDP)

Foraminiferal species of *Kurnubia palastiniensis*, *Nautiloculina oolithica*, and *Alveosepta jaccardi* are the dominant constituent grains for the foraminiferal wackestone/mud-dominated packstone facies, whereas *Redmondoides lugeoni* and *Lenticulina sublenticularis* species are rarely present (Fig. 7D). The foraminiferans are very fine to coarse grained and are supported by carbonate mud. They generally have micritized tests by which they can be recognized from their preserved microstructures. Other grains associated with the foraminifera include brachiopods, echinoid spines and plates, and rarely quartz grains. In the outcrop, the foraminiferal facies is characterized by yellowish-brown color and extensive bioturbation (Fig. 7). Based on Taylor and Goldring's (1993) bioturbation index (BI) scheme, a BI of 5 – 6 is recognized based on the obliteration of bedding by *Planolites* and *Thalassinoides* burrows.

The foraminiferal assemblage (Hughes, 2004) and other fauna present represent an open-marine depositional setting below FWWB. This interpretation is also supported by the intensive bioturbation, as Knaust et al. (2012) suggested that moderate to high bioturbation by *Cruziana* ichnofacies, which *Planolites* and *Thalassinoides* belong to, indicates a shallow-marine depositional environment between FWWB and storm wave

base (SWB). Knaust (1998) also demonstrated that the higher degree of bioturbation in the Lower Muschelkalk of Germany is indicative of outer ramp setting. In a shallowing-upward succession, the skeletal and peloidal grainstone facies overlies this facies. As a result, proximal lower shoreface environment is interpreted for the foraminiferal facies.

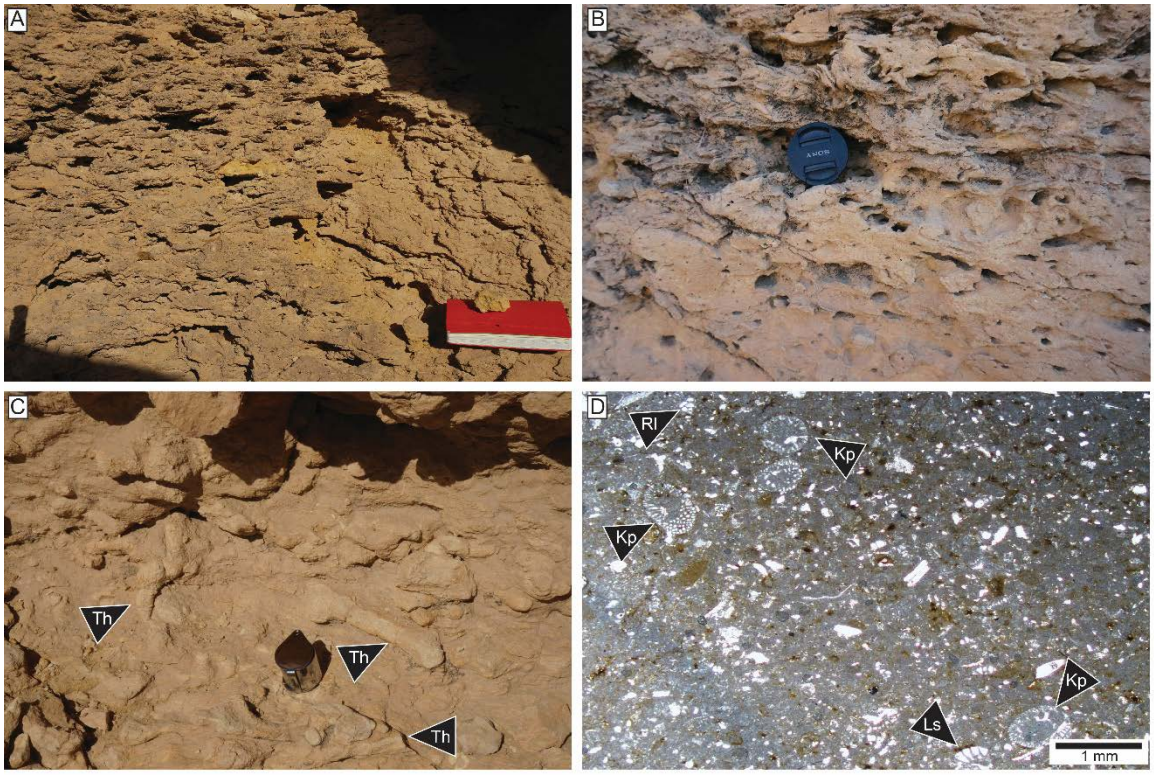

Fig. 7. Bioturbated foraminiferal wackestone/mud-dominated packstone facies. (**A**) The foraminiferal facies is characterized by homogenized appearance related to extensive bioturbation [notebook = 21 cm]. (**B**) Close-up view showing total destruction of bedding planes [lens cap = 4 cm]. (**C**) Highlighted *Thalassinoides* burrows [Th] within the foraminiferal wackestone/mud-dominated packstone. (**D**) Photomicrograph under plane-polarized light showing a wackestone with the foraminifera species *Kurnubia palastiniensis* [Kp], *Redmondoides lugeoni* [Rl], and *Lenticulina sublenticularis* [Ls].

ONCOLITIC RUDSTONE

Oncoids, as large as 1 cm, are observed in massive, medium to thick beds (45 – 95 cm) of rudstone texture. Their grain size range is 1.3 – 6.6 mm and they are characterized by bioclastic nuclei consisting of mollusks, brachiopods, foraminifera, or corals (Figs. 8C, 8D, and 8E). The shape of the oncoids generally follows their nuclei, but they also grow into lobate shapes. The cortices are defined by micritic and organism-encrusted laminae, which are made by *Bacinella irregularis* and *Lithocodium aggregatum* microencrustors. Type 3 oncoids (Védrine et al., 2007) are the dominant type where cortices are defined by alternating micritic laminae and organism-bearing laminae (Fig. 8D). Other types of oncoids occur sporadically, which includes types 1 (oncoids of micritic cortices with poorly-defined lamination) and type 2 (oncoids of irregular and truncated micritic laminae) (Védrine et al., 2007). Besides the oncoids, other constituent grains present in this facies consist of foraminifera (*Kurnubia palastiniensis*, *Nautiloculina oolithica*, and *Alveosepta jaccardi)*, brachiopod fragments, peloids, intraclasts, and echinoderms. These grains are observed in association with micrite forming mud-dominate/grain-dominate packstone (Fig. 8D). Pebble-size fragments of corals and stromatoporoids can be observed within the oncolitic matrix. Moreover, sparse, isolated coral heads in growth position are also recognized within the oncolite beds (Fig. 8B).

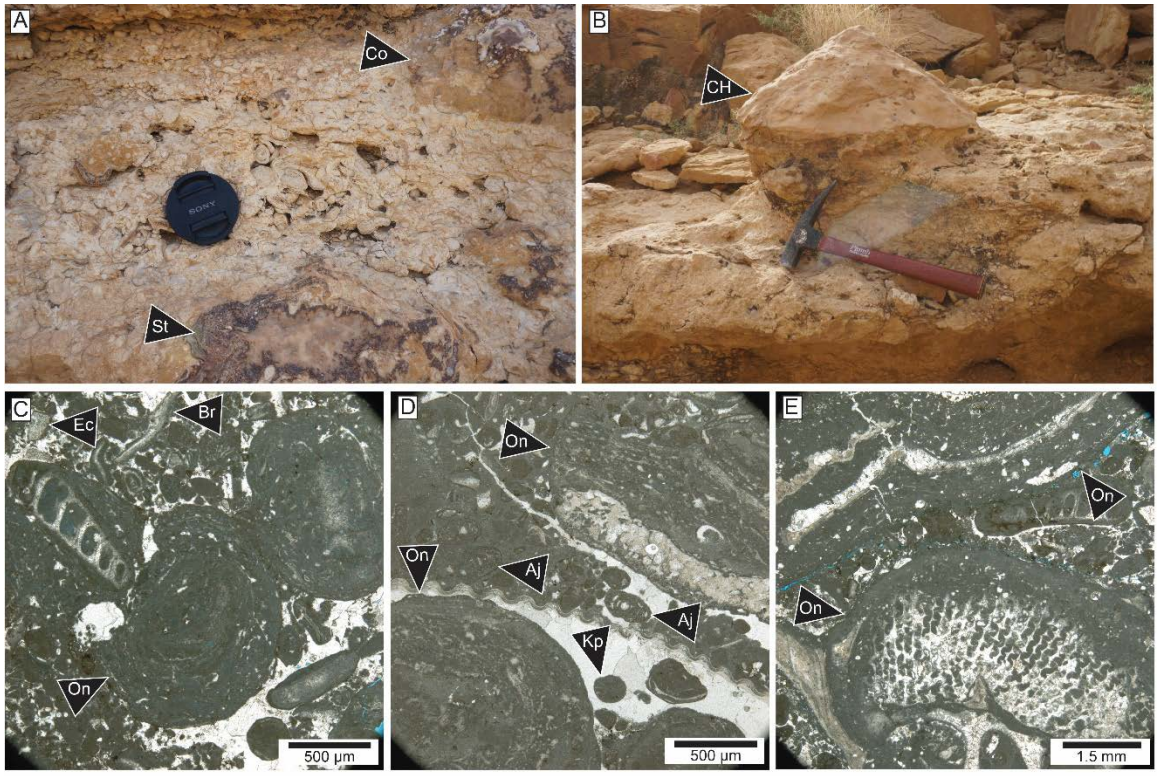

Fig. 8. Oncolitic rudstone facies. (**A**) Oncolitic facies has massive beds with floating fragments of corals [Co] and stromatoporoids [St] [lens cap = 4 cm]. (**B**) Some isolated coral heads [CH] are observed in growth position within the oncolitic matrix [hammer = 30 cm]. (**C**) Photomicrograph under plane-polarized light showing a poorly-sorted fabric of oncoids [On] and fragments of echinoderms [Ec] and brachiopods [Br]. (**D**) Photomicrograph under plane-polarized light showing the *Bacinella – Lithocodium* meshwork on the oncoids [On] cortices. This facies also contains foraminifera species *Kurnubia palastiniesis* [Kp] and *Alveosepta jaccardi* [Aj]. (**E**) Nuclei of the oncoids [On] are either composed of corals, brachiopods, mollusks, or foraminifera [photomicrograph under plane-polarized light].

Type 3 *Bacinella – Lithocodium* oncoids are indicative of low-energy settings with low accumulation rates (Védrine et al., 2007). The faunal assemblage and corals growth in association with this facies suggest normal open-marine conditions, and thus, the depositional environment is interpreted to be below FWWB. This is also supported by the presence of micrite and lobate growth of the oncoids (Flügel, 2010). Because the oncolitic

rudstones are commonly observed below the foraminiferal facies in a shallowing-upward succession, their depositional environment is assigned to the proximal lower shoreface.

STROMATOPOROID-CORAL BIOSTROME/BIOHERM

Stromatoporoids and corals of the Hanifa Formation form two styles of stratigraphic reefs, either biostromes or bioherms (James and Jones, 2015). The biostromes are well-bedded with medium to very thick beds of 15 – 150 cm, whereas the bioherms are massive and poorly bedded with a thickness range of 1.5 – 11 m (Fig. 9). Another characteristic of the biostromes is that they are commonly interbedded with the spiculitic facies, described below, and are laterally continuous. Furthermore, both biostromes and bioherms are predominantly characterized by *in-situ* isolated coral and stromatoporoid heads with a micritic matrix and may have microbial and stromatoporoid encrustation (Figs. 9F and 9G). Based on the extensive description of the Hanifa corals by El-Asa'ad (1991), and El-Sorogy and Al-Sahtany (2015), the corals have hemispherical or globular forms. Some of the identified species include *Latiastrea greppini*, *Synastrea delemontana*, *Coenastraea abakkaynata*, *Microphyllia sommeringi*, and *Koilomorpha hanifaensis* (Figs. 9C and 9D).

The depositional environment of the stromatoporoid-coral biostromes is assigned to the distal lower shoreface as they are generally overlain by the oncolitic facies in a shallowing-upward succession. Such a low-energy environment is interpreted based on the muddy spiculitic matrix and low frequency of storm deposits. This interpretation is in general agreement with that of Olivier et al. (2011) and Kästner et al. (2008) where they interpreted the depositional setting of the French Jura corals and the Korallenoolith coral biostromes, respectively, below FWWB. Conversely, the stromatoporoid-coral bioherms are interpreted to have been deposited in the proximal lower shoreface environment above FWWB. The presence of hemispherical and globular corals without solitary nor branching forms suggests a high-energy environment (El-Asa'ad, 1991).

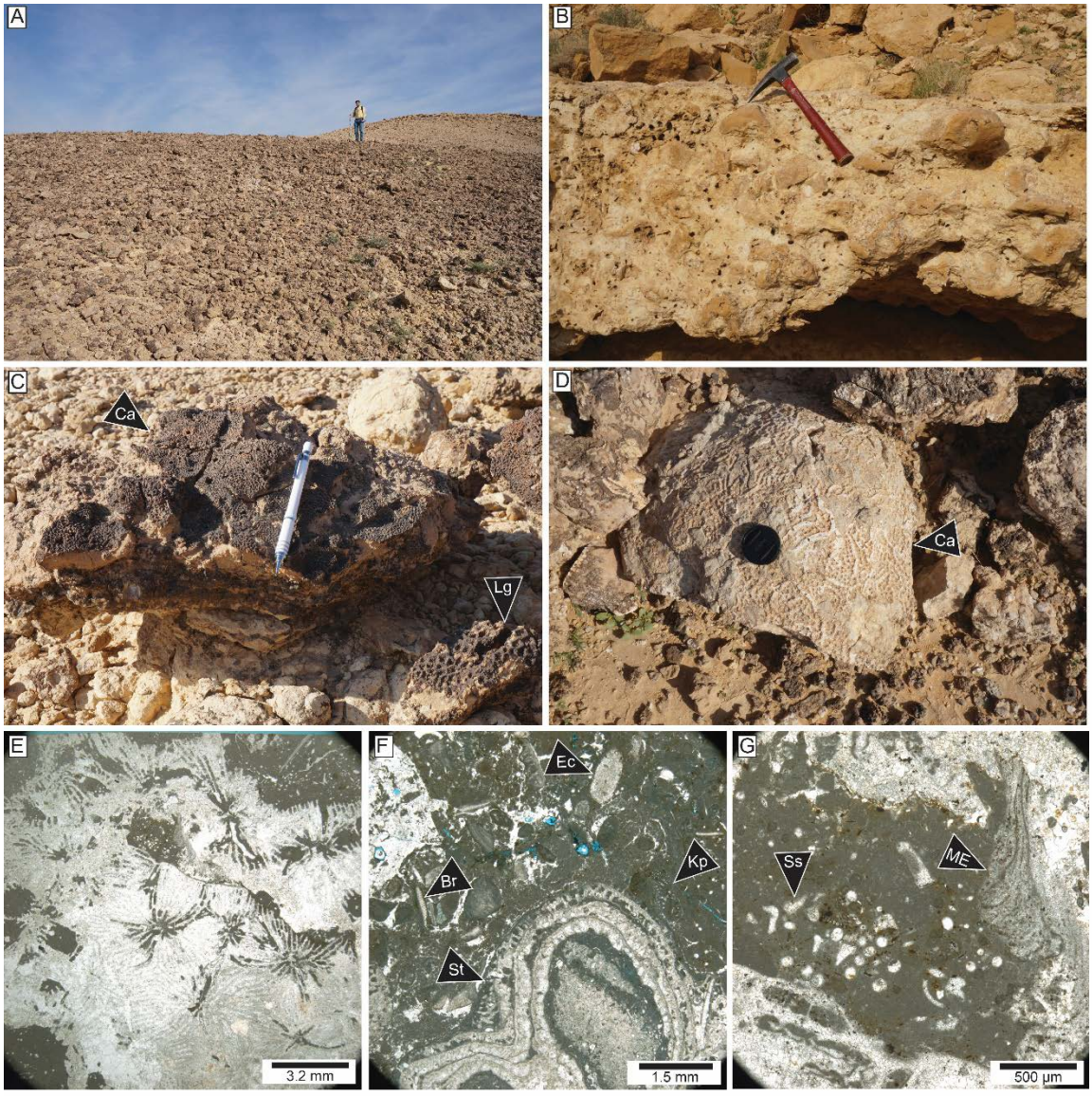

Fig. 9

Fig. 9. Stromatoporoid-coral biostrome/bioherm facies. (**A**) The general expression of the biohermal stromatoporoids and corals buildups is characterized by scattered coral rubbles related to the micritic matrix differential weathering. (**B**) The stromatoporoids-corals biostromes are well-indurated and show coral heads in their growth positions [hammer = 30 cm]. (**C**) Two in-situ coral species: *Coenastraea abakkaynata* [Ca] and *Latiastrea greppini* [Lg] [pencil = 15 cm]. (**D**) A *Coenastraea abakkaynata* (Ca) coral in growth position [lens cap = 4 cm]. (**E**) Photomicrograph under plane-polarized light showing coral septa where cavities are filled with micrite. (**F**) Photomicrograph under plane-polarized light of an encrusting stromatoporoids [St] within a micritic matrix, which includes the foraminifera species *Kurnubia palastiniensis* [Kp], brachiopods [Br], and echinoderms [Ec]. (**G**) Sponge spicules [Ss] are abundant within the micritic matrix, whereas microbial encrustation [ME] is common for this facies [photomicrograph under plane-polarized light].

PELOIDAL/COMPOSITE-GRAIN GRAIN-DOMINATED PACKSTONE (GDP)/GRAINSTONE

Peloids and composite-grains within the grain-dominated packstone to grainstone are the primary grain types for this facies in the Hanifa and Jubaila Formations. The peloidal GDP/grainstone facies in the Hanifa Formation is dominated by very well-sorted, very-fine grains of peloids, micritized *Redmondoides lugeoni* foraminifera, and sparse echinoderm fragments (Fig. 10). Rip-up clasts and coral fragments of granule to pebble-size are common and generally observed accumulated at the base of some of the beds. These beds can be characterized as thin to thick beds (5 – 90 cm) with normal grading, and display planar and low-angle lamination (4^o – 10^o), or hummocky cross-stratification (Fig. 10A). Also, a low degree of bioturbation (BI = 2; Taylor and Goldring, 1993) is common where bedding surfaces and laminations are preserved (Fig. 10D).

These features are well-illustrated in the equivalent beds of the Jubaila Formation where there is a strong differentiation between two styles of sedimentation (Fig. 10B vs. 10C). Beds of the first style are observed interbedded with the bioturbated echinoderm-brachiopod wackestone/mud-dominated packstone facies that is described below. They are characterized by thin to thick beds of 5 – 35 cm and primarily composed of moderately- to well-sorted, medium to very coarse grains of composite grains. Other constituents include

micritized *Kurnubia palastiniensis* and *Alveosepta jaccardi* foraminifera, and fragments of brachiopods and echinoids. The beds are also distinctively characterized by erosional basal surfaces where granule to pebble size mud-clasts from the underlying units are incorporated at the base of the beds. Conversely, the upper surface is sharp and might be a hardground, or mega-rippled surface (Fig. 10B). The mega-ripples are characterized by 60 – 100 cm wavelengths and 5 – 15 cm wave heights. Moreover, bed tops are commonly bioturbated by the horizontal burrows *Planolites* and *Rhizocorallium* (Figs. 10E and 10F). Although these beds are also burrowed by *Thalassinoides*, bioturbation is considered to be low as indicated by the preservation of the sedimentary structures (Fig. 10D). In addition to the mega-ripples, planar lamination, low-angle lamination (4^o – 8^o) and hummocky cross-stratification within the beds are also present.

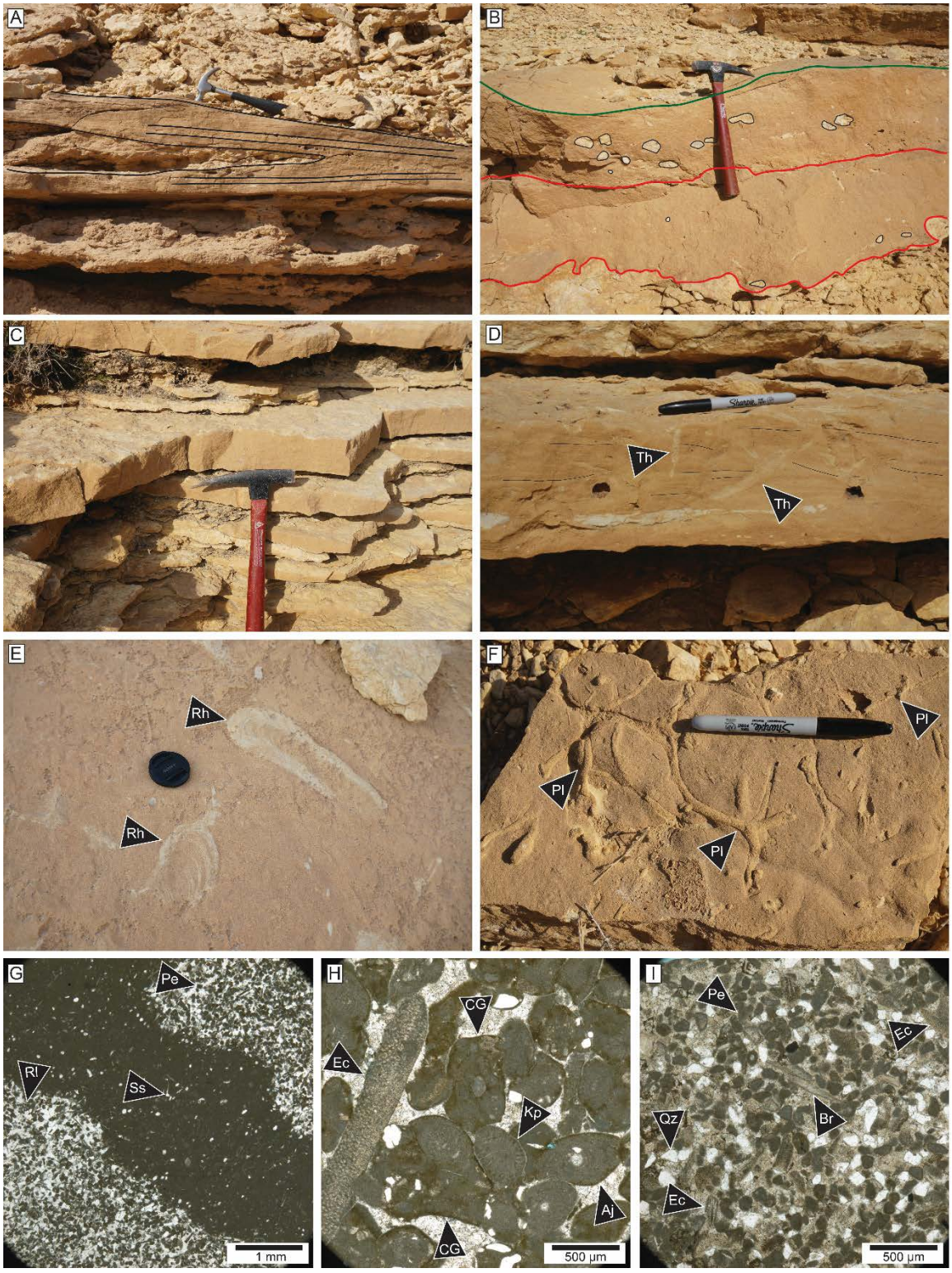
A
B
C
D
Th
Th
E
Rh
Rh
F
Pl
Pl
Pl
G
Pe
Rl
Ss
1 mm
H
CG
Ec
Kp
Aj
CG
500 µm
I
Pe
Ec
Qz
Br
Ec
500 µm

Fig. 10

Fig. 10. Peloidal/composite-grain grain-dominated packstone/grainstone facies (tempestites). (**A**) Tempestite bed interbedded with bioturbated muddy sediments displays hummocky cross-stratification [hammer = 26 cm]. (**B**) Proximal tempestites commonly have erosional bases [red lines] associated with rip-up clasts from the underlying units. Another feature to proximal tempestites is the amalgamation of multiple event beds, and may develop megarippled top surfaces [green line] [hammer = 30 cm]. (**C**) Distal tempestites are thinner than proximal equivalents and have sharp planar basal and upper surfaces [hammer = 30 cm]. (**D**) A low degree of bioturbation is a common feature of the event beds, although they are burrowed by *Thalassinoides* [Th]. The intensity of bioturbation is low given the preservation of bedding surfaces and internal lamination [black lines] [pen = 14 cm]. (**E**) Horizontal burrows are the dominant trace fossils and observed on the top surface of the temepstites, such as *Rhizocorallium* [Rh] [lens cap = 4 cm]. (**F**) Network of *Planolites* [Pl] burrows on top of a storm bed [pen = 14 cm]. (**G**) Photomicrograph under plane-polarized light of a very well-sorted peloidal [Pe] and foraminiferal (*Redmondoides lugeoni* [Rl]) grainstone showing a burrow cavity filled with micrite and sponge spicules [Ss]. (**H**) Proximal tempestites have moderately sorted fabric dominated by coarse size composite grains [CG], echinoderms [Ec], and foraminifera species *Kurnubia palastiniensis* [Kp] and *Alveosepta jaccardi* [Aj] [photomicrograph under plane-polarized light]. (**I**) The distal tempestites are characterized by finer grain size, in which peloids [Pe], echinoderms [Ec], quartz [Qz], and brachiopods [Br] are the dominant grains [photomicrograph under plane-polarized light].

By contrast, beds of the second style are very thinly to thinly bedded (2 – 8 cm) and have sharp planar basal and upper contacts (Fig. 10C). Their main sedimentary structures are planar or low-angle (~4^{o}) lamination. In terms of composition, they are composed of moderately to well-sorted, very fine to fine peloids, echinoderm fragments, brachiopods and subangular to subrounded quartz grains. Quartz grains form 10 – 20% of the sediments and may compose 40% of the deposit. Nevertheless like the first style of sedimentation, beds of the second depositional style have horizontal burrows on their top surfaces as well as interbedding with the extensively bioturbated echinoderm-brachiopod wackestone/mud-dominated packstone facies.

The lower shoreface environment was the depositional setting for the peloidal/composite-grain facies of the Hanifa and Jubaila Formations. The features

supporting this interpretation include the style of bedding, type of bedding contacts, sedimentary structures, and ichnofabrics. Thicker beds with erosional bases represent proximal storm-event beds (tempestites) whereas thinner beds with sharp bases are distal tempestites. As Aigner (1985, 1982) illustrated, proximal tempestites have erosional bases, wave-rippled tops, and composed of coarse grains. In contrast, distal tempestites are relatively thinner and contain finer sediments. The hummocky cross-stratification (Dumas and Arnott, 2006), and *Planolites* and *Rhizocorallium* of the *Cruziana* ichnofacies (Knaust et al., 2012) are indicative of depositional settings between FWWB and SWB. The Jurassic tempestites of Kachchh of western India also show the same relationship between storm beds and the *Cruziana* ichnofacies (Fürsich, 1998).

BIOTURBATED ECHINODERM-BRACHIOPOD WACKESTONE/MUD-DOMINATED PACKSTONE

The bioturbated echinoid-brachiopod wackestone/mud-dominated packstone facies is encountered within basal Jubaila Formation in which extensive bioturbation (BI = 5 – 6; Taylor and Goldring, 1993) resulted in a complete destruction of bedding. The burrows reflect the *Cruziana* ichnofacies (Knaust et al., 2012), with traces of *Thalassinoides*, *Planolites*, *Rhizocorallium*, and *Condrites* are recognized in the outcrop (Fig. 11). Internally, the facies is composed of poorly sorted fragments of brachiopods and echinoderms, forming wackestone to mud-dominated packstone textures. Other constituents include mollusks, sparse sponge spicules, foraminifera, and subangular to subrounded fine-sized quartz grains. Detrital quartz grains, when present, form about 5 – 10% of the facies.

The faunal assemblage recognized in this facies suggests normal open-marine conditions. Deposition took place in a low-energy setting between FWWB and SWB on the basis of extensive bioturbation by the *Cruziana* ichnofacies (Fürsich, 1998; Knaust, 1998; Knaust et al., 2012). This setting corresponds to the lower shoreface environment since deposition of this facies had been intermittently disrupted by storm event beds.

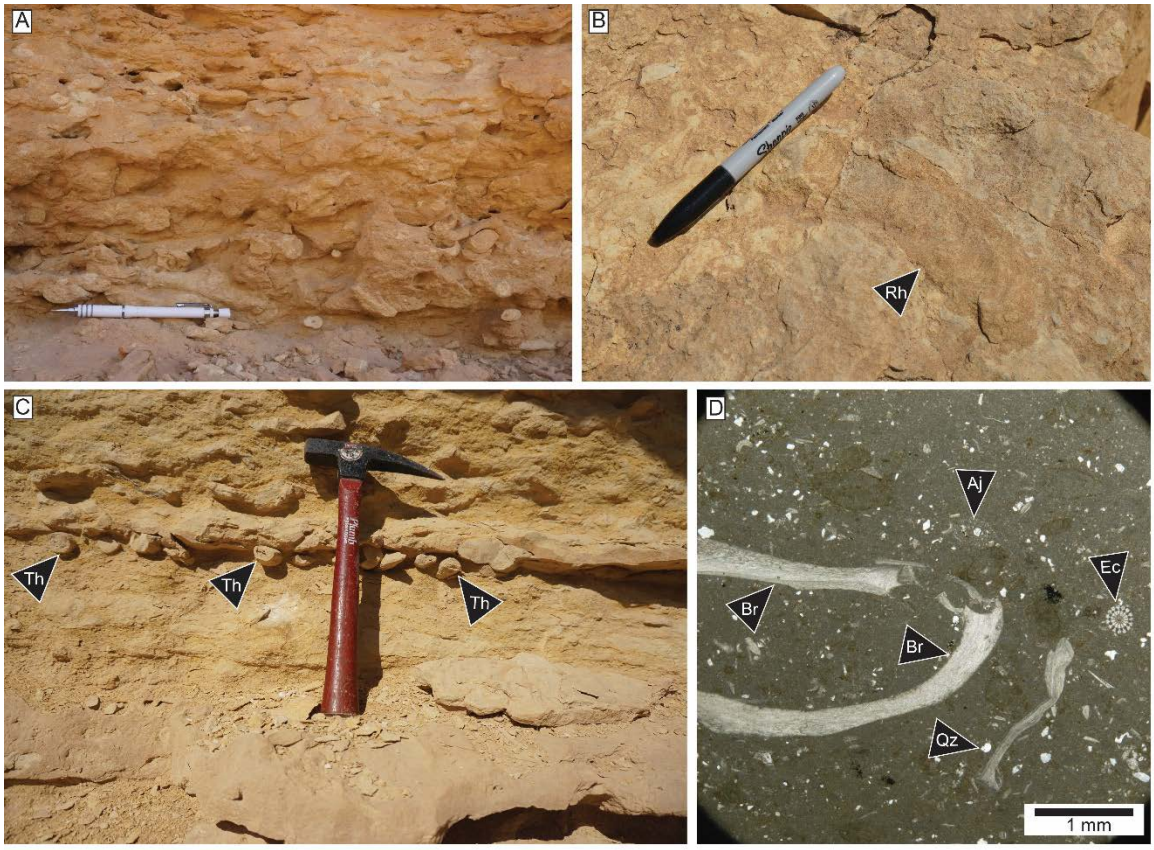

Fig. 11. Bioturbated echinoderm-brachiopod wackestone/mud-dominated packstone facies. (**A**) Extensive bioturbation resulted in complete obliteration of bedding [pencil = 15 cm]. (**B**) *Rhizocorallium* [Rh] burrow highlighted on an exposed surface [pen = 14 cm]. (**C**) Burrows also include *Thalassinoides* [Th] as shown by their casts beneath a thin tempestite [hammer = 30 cm]. (**D**) Photomicrograph under plane-polarized light showing a very poorly-sorted fabric with brachiopods [Br], echinoderms [Ec], foraminifera species *Alveosepta jaccardi* [Aj], and quartz [Qz] forming a wackestone units.

BIOTURBATED SPICULITIC WACKESTONE/MUD-DOMINATED PACKSTONE

Abundant sponge spicules are the dominant grain types of the bioturbated spiculitic facies that create wackestone to mud-dominated packstone where carbonate mud composes 60 – 80% of the fabric. Besides the spicules, the facies consists of foraminifera, echinoderms, and sparse fragments of mollusks and brachiopods. The sponge spicules are

mainly monaxons and triaxons that sporadically have their central canal preserved, which suggests they are likely siliceous originally (Scholle and Ulmer-Scholle, 2003; Figs. 12C and 12D). In the outcrop, the facies is characterized by grayish white color and friable outcrop quality. This fabric is probably a product of differential compaction and high to intense bioturbation (BI = 4 – 5) by *Planolites*, which resulted in nodular bedding with irregular, wavy, and nonparallel bedding surfaces (Fig. 12A). In addition, the spiculitic facies is commonly associated with hardground and firmground surfaces and contains storm event beds sporadically throughout.

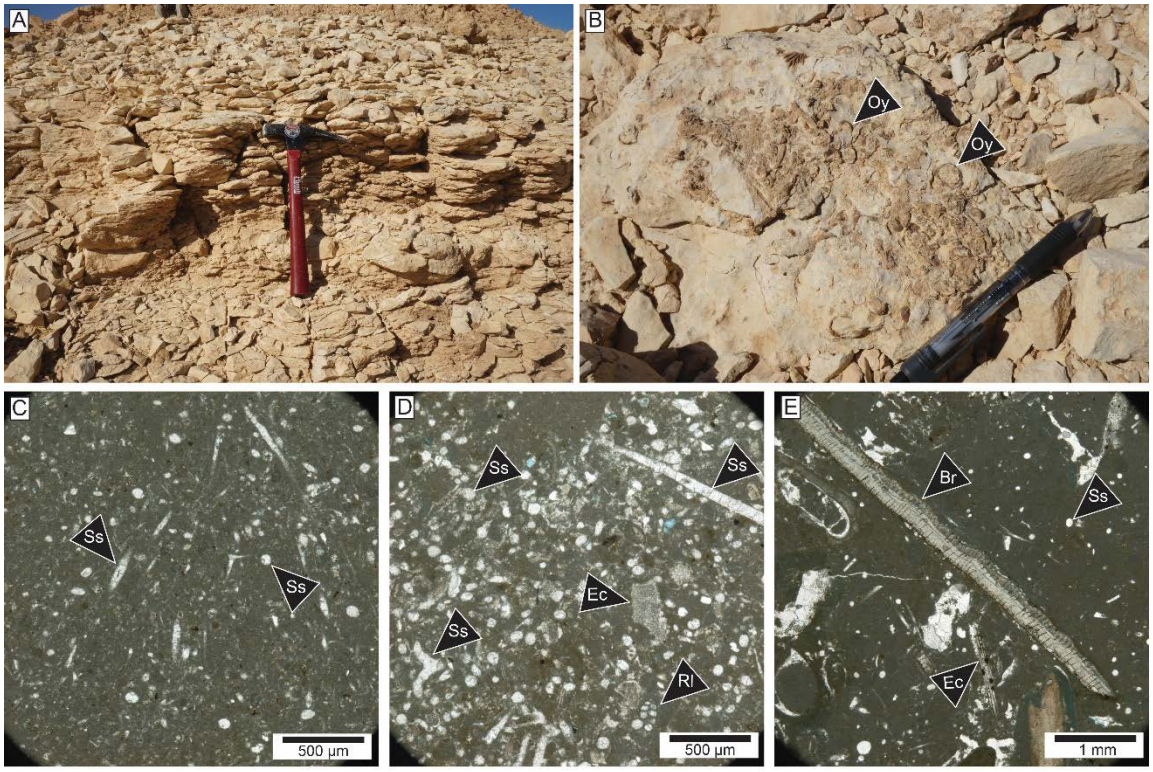

Fig. 12. Bioturbated spiculitic wackestone/mud-dominated packstone facies. (**A**) The facies is characterized by crumbly appearance and nodular bedding produced by bioturbation [hammer = 30 cm]. (**B**) Hardground surface encrusted with oysters [Oy] [pen = 15 cm]. (**C**) Sponge spicules [Ss] in a micritic matrix. (**D**) Mud-dominated packstone with sponge spicules [Ss], echinoids [Ec], and the foraminifera species *Redmondoides lugeoni* [Rl]. (**E**) Photomicrograph of wackestone with sponge spicules [Ss], echinoids [Ec], and brachiopods [Br].

The abundance of carbonate mud in the spiculitic facies indicates a low-energy depositional setting. Based on the faunal assemblage, particularly the sponge spicules (Hughes, 2004), bioturbation, and interbedding with tempestites, normal open-marine conditions between FWWB and SWWB is interpreted for this facies. In a shallowing-upward succession of the Hanifa, the coral biostrome facies overlies the spiculitic facies, and therefore, the depositional environment of the spiculitic facies is interpreted to be the distal lower shoreface. This interpretation is consistent with that made by Kästner et al. (2008) where they reported a similar facies in a depositional setting between FWWB and SWWB.

THINLY-BEDDED ARGILLACEOUS MUDSTONE/WACKESTONE

The argillaceous mudstone/wackestone facies is exposed as recessive slopes that can be traced across the entire outcrop belt. The best exposures of this facies are on roadcuts where the characteristics of the deposits are well-defined (Fig. 13). The most striking character of this facies is the alternation of thin beds (5 cm thick) of spiculitic mudstone/wackestone and clay-rich beds. Spiculitic wackestones increase progressively thicken upward and become medium bedded (20 cm thick) at the expense of clay.

The depositional setting for the argillaceous limestone is interpreted to be the offshore environment below SWB. The dominance of carbonate mud and argillaceous materials supports this interpretation. Furthermore, stressed environmental conditions, likely related to low oxygenation levels, inhibited burrowing organisms and diverse faunal assemblages that resulted in the preservation of discrete bedding surfaces. The same interpretation was also concluded by Carlucci et al. (2014) for their thinly bedded mudstone and shale facies.

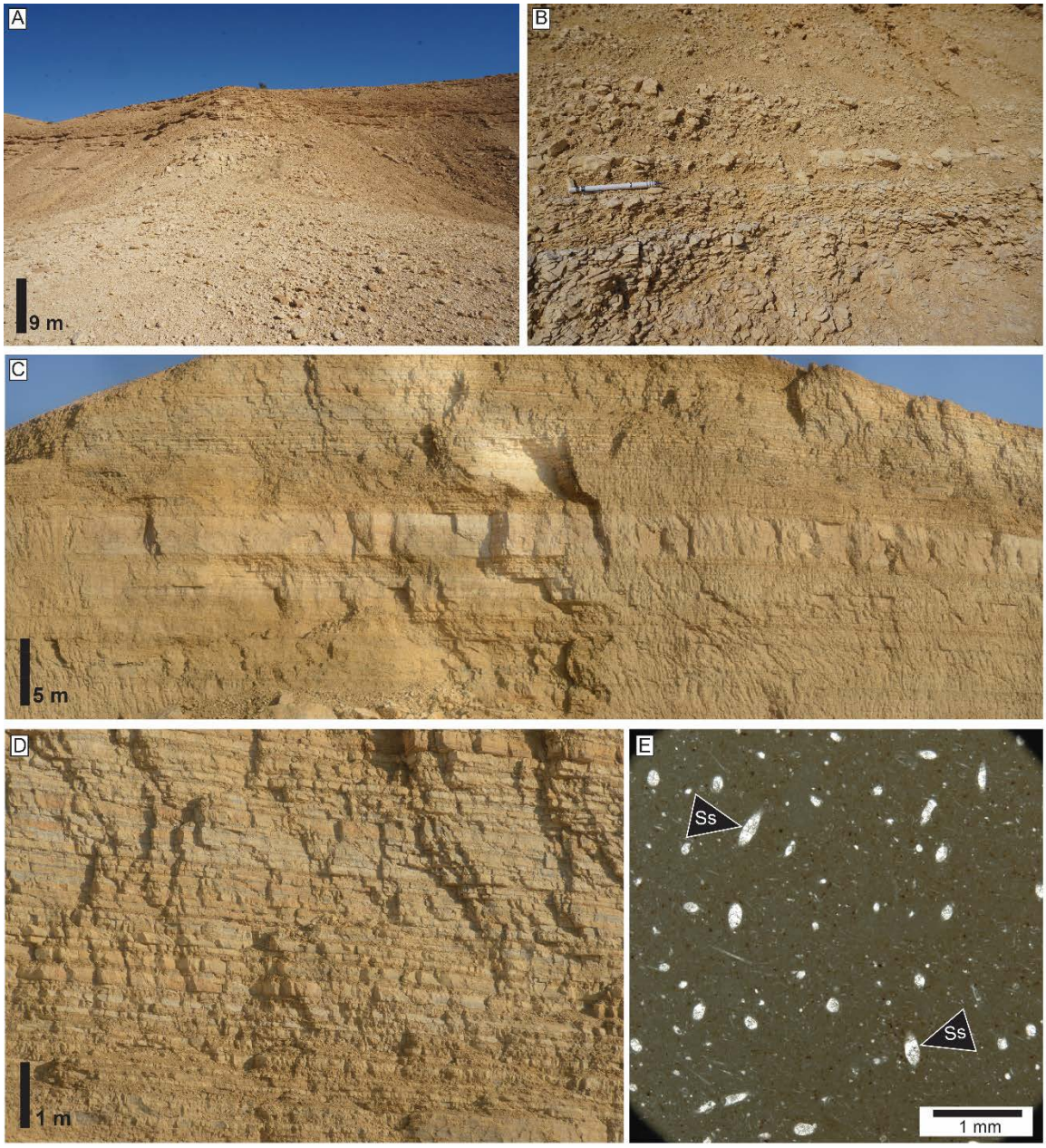

Fig. 13

Fig. 13. Thinly-bedded argillaceous mudstone/wackestone facies. (**A**) The argillaceous facies is commonly poorly exposed and forms recessive slopes. (**B**) A close-up view of the argillaceous facies demonstrating the general poor exposure. (**C**) Roadcuts along the Tuwaiq Escarpment have fresh exposures that allow observing the depositional style of alternating recessive argillaceous mudstones and resistive wackestones. (**D**) Close-up view of roadcut section showing thinly-bedded alternation of argillaceous mudstones [yellowish brown] and wackestones [yellowish white]. (**E**) Photomicrograph showing a wackestone dominated by sponge spicules [Ss].

SEQUENCE STRATIGRAPHIC FRAMEWORK OF THE HANIFA FORMATION

The regional cross-section of the Hanifa Formation illustrates the temporal and spatial facies distribution along the Tuwaiq Escarpment (Fig. 14). Overall, the Hanifa framework depicts a ramp profile where timelines are gently dipping to the south. Following the same trend, a progressive thickening of the Hanifa Formation from 86 m at the Raghbah section in the north to 143.5 m at the Wadi Birk section in the south over a distance of 260 km is also apparent (Fig. 14). Moreover, the number of the preserved Hanifa depositional sequences was also affected by this trend. The Hanifa Formation could be divided into five composite sequences that are best represented in the southern part of the study area (Fig. 14). However, only four composite sequences can be interpreted from the sections in the northern end of the area.

The first sequence (Seq1) is only observed in the south at the Hawtah and Wadi Birk sections (Abdullah Al-Mojel's measured sections). It marks the initial transgression of the Hanifa Formation over the Tuwaiq Mountain Limestone, on which it onlaps. The dominant facies of the sequence are the argillaceous mudstone/wackestone and stromatoporoid-coral biostrome/bioherm facies. The transgression of the sequence, and the Hanifa Formation, is defined by the deposition of the thinly-bedded argillaceous mudstone/wackestone facies, which is thicker at the Wadi Birk section and thins northward towards the Hawtah section. Conversely, the stromatoporoid-coral facies thins southward towards the Wadi Birk section. The sequence boundary for Seq1 is picked on top of the stromatoporoid-coral facies based on sharp facies offset with the overlying argillaceous mudstone/wackestone facies that define the transgression of the next composite sequence. This transgression probably eroded the shallow-water facies of the first sequence.

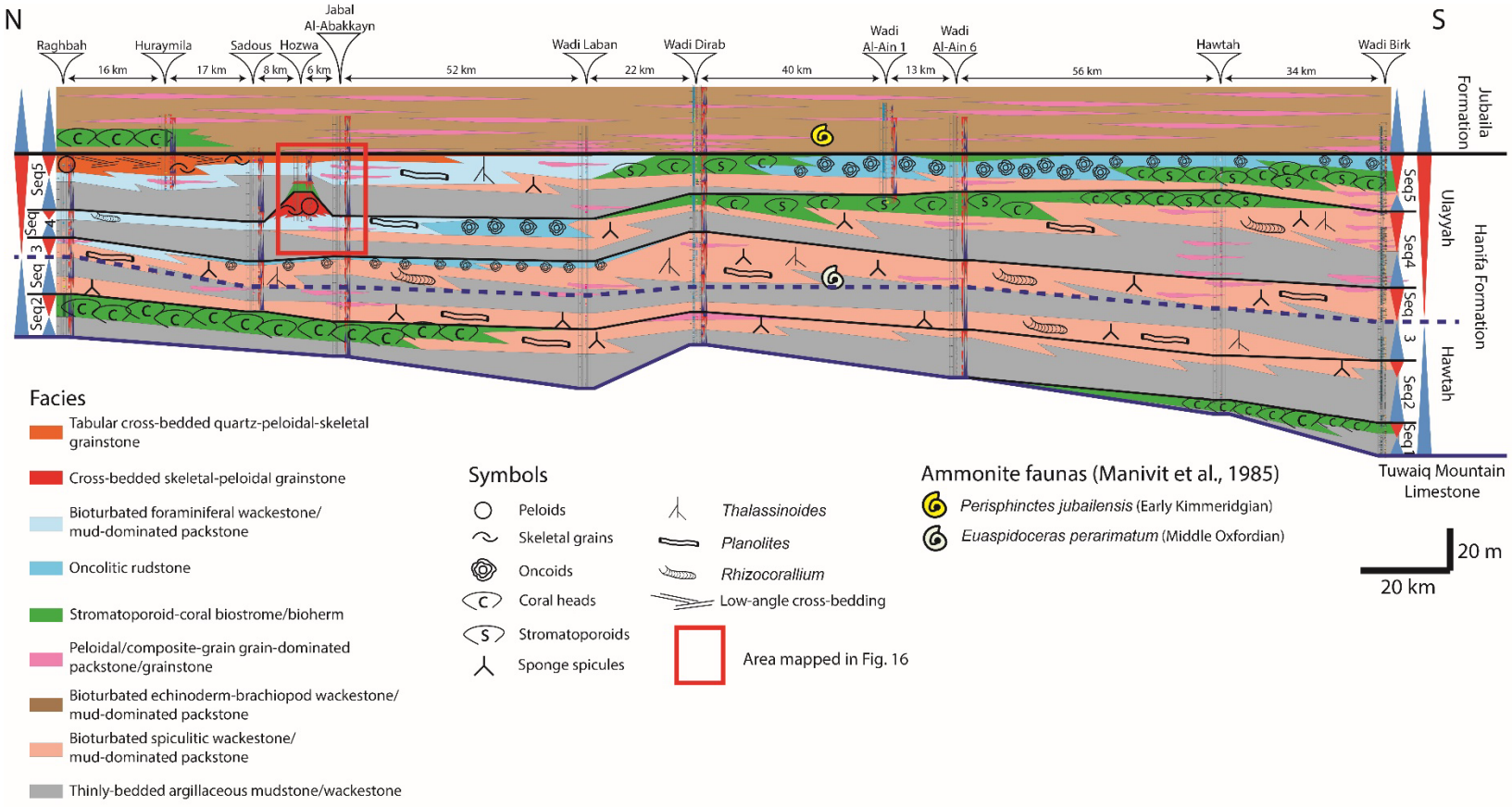

Fig. 14. Cross-section showing the sequence stratigraphic framework of the Hanifa Formation datumed on the Hanifa-Jubaila contact. The formation is divided into five composite sequences in the south, whereas in the north, the fifth sequence is not present. The contact with the Jubaila Formation is defined by a sharp contact marking the onset of a storm-dominated shelf associated with the Jubaila transgression.

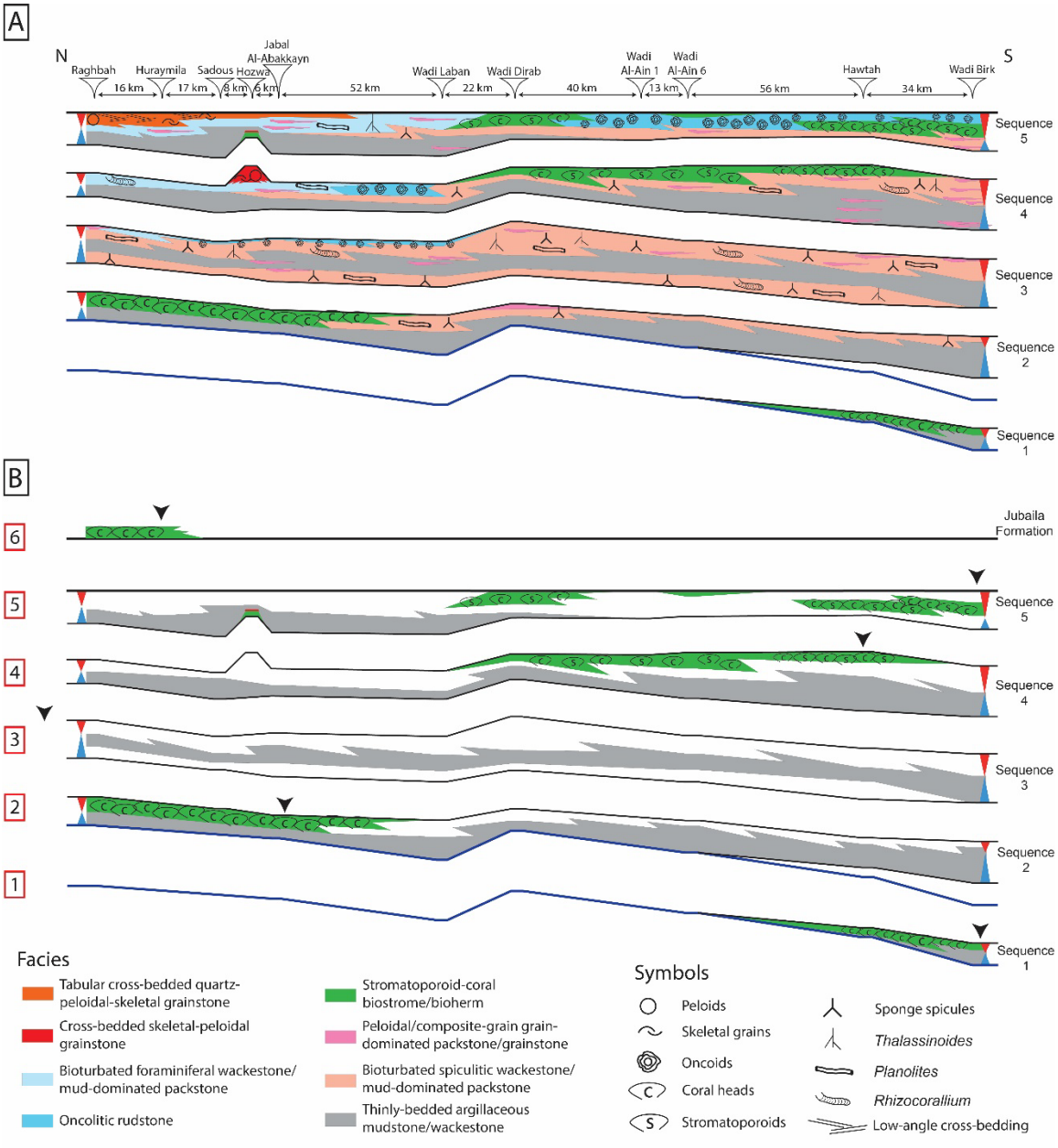
A
N
S
Raghbah
Huraymila
Sadous
Jabal Al-Abakkayn
Hozwa
Wadi Laban
Wadi Dirab
Wadi Al-Ain 1
Wadi Al-Ain 6
Hawtah
Wadi Birk
16 km
17 km
8 km
6 km
52 km
22 km
40 km
13 km
56 km
34 km
Sequence 5
Sequence 4
Sequence 3
Sequence 2
Sequence 1
B
6
5
4
3
2
1
Jubaila Formation
Sequence 5
Sequence 4
Sequence 3
Sequence 2
Sequence 1
Facies
Tabular cross-bedded quartz-peloidal-skeletal grainstone
Cross-bedded skeletal-peloidal grainstone
Bioturbated foraminiferal wackestone/ mud-dominated packstone
Oncolitic rudstone
Stromatoporoid-coral biostrome/bioherm
Peloidal/composite-grain grain-dominated packstone/grainstone
Bioturbated spiculitic wackestone/ mud-dominated packstone
Thinly-bedded argillaceous mudstone/wackestone
Symbols
Peloids
Skeletal grains
Oncoids
Coral heads
Stromatoporoids
Sponge spicules
Thalassinoides
Planolites
Rhizocorallium
Low-angle cross-bedding

Fig. 15

Fig. 15. (**A**) Individual composite sequences of the Hanifa Formation showing depositional variations spatially through time. The base of sequences 1 and 2 is the top of the Tuwaiq Mountain Limestone. Shallow-water, high-energy deposits of sequence 1 were most likely eroded with the transgression of sequence 2. (**B**) The Hanifa Formation corresponds to a single second-order sequence interpreted based on the relative lateral position of the stromatoporoid-coral biostrome/bioherm facies through six depositional sequences. Black arrows mark the farthest downdip position of the coral facies in a measured section. The argillaceous mudstone/wackestone facies are associated with transgression of each Hanifa composite sequence. At time 3, the coral facies continued to retrograde north of the study area, marking the maximum flooding surface of the Hanifa Formation.

The second sequence (Seq2) extends over the entire study area where transgression is marked by laterally continuous argillaceous mudstone/wackestone facies at the base of Seq2, which thins to the north. At the top of the sequence, the spiculitic facies covers the area from Wadi Birk in the south, where they are much thinner, to Wadi Laban in the north. The lateral equivalent facies to the north is the stromatoporoid-coral facies. Its northerly position in this sequence, relative to that in Seq1, illustrates the back-stepping character, while stromatoporoid-coral buildups were trying to keep pace with the ongoing transgression (Figs. 14 and 15). Above the coral facies, the Seq2 sequence boundary is picked based on sharp facies offset with the spiculitic facies of the next sequence. To the south, the sequence boundary of Seq2 is inferred from the change in facies proportion where the ratio of argillaceous mudstone/wackestone facies to spiculitic facies increases.

At the base of the third composite sequence (Seq3), the ratio of argillaceous mudstone/wackestone facies relative to spiculitic facies increases upward towards the maximum flooding surface of the sequence where it becomes prominent. The spiculitic facies dominates the highstand portion of the sequence, which displays an upward shallowing succession north of Wadi Dirab to a combination of oncolitic and foraminiferal facies. Similar to Seq1, the sequence boundary for Seq3 is interpreted based on sharp facies offset at the base of the transgressive argillaceous mudstone/wackestone of the fourth sequence (Seq4).

The highstand part of Seq4 shows the lateral facies juxtaposition of the Hanifa depositional profile (Figs. 14 and 15). The stromatoporoid-coral facies extends from Wadi Dirab to Hawtah where biostromal units at the sections of Wadi Dirab and Wadi Al-Ain occur. At the Hawtah section, bioherms occur that laterally pass downdip into the spiculitic facies at Wadi Birk. To the north, the stromatoporoid-coral facies is laterally equivalent to the oncolitic and foraminiferal facies updip. These lateral facies changes are gradual and occur over long distances. The only exception to this is the area near the Hozwa section where a rapid lateral facies change occurs (Figs. 14 and 16). At Hozwa the foraminiferal facies becomes laterally equivalent to the cross-bedded skeletal-peloidal grainstone facies (Fig. 16). This unusual rapid lateral facies change for the studied system is unique to the Hozwa area where the cross-bedded skeletal-peloidal grainstone facies occurs and is about 12 – 15 m thick. Also in this area, the top of Seq4 is uniquely defined by a karst-modified unconformity surface (Fig. 17). The top of the cross-bedded peloidal grainstones exhibits an erosional relief of up to two meters. Solution pipes on the unconformity surface are also recognized (Fig. 17D). Laterally, the unconformity surface is equivalent to hardground surfaces at Sadous, Jabal Al-Abakkayn, and Wadi Dirab sections. Besides the unconformity, the Seq4 sequence boundary is also recognized by sharp facies offset with the argillaceous mudstone/wackestone facies of the fifth sequence (Seq5).

The argillaceous mudstone/wackestone facies defines the transgression of Seq5 along the outcrop belt, whereas transgression in the Hozwa area is marked by widespread nucleation of coral buildups on top of the cross-bedded peloidal grainstones (Fig. 17). These buildups are laterally equivalent to the thinly-bedded argillaceous mudstone/wackestone facies that pinches out against the buildups (Fig. 16). During the highstand of Seq5, the stromatoporoid-coral facies prograded southward to Wadi Birk. The coral facies at Wadi Birk and Wadi Al-Ain have biohermal geometries, whereas the coral facies at Wadi Dirab are biostromal. The filling of the area between Wadi Birk and Wadi Dirab by the oncolitic facies is also notable. To the north, the lateral equivalent to the coral and oncolite facies are the foraminiferal and tabular cross-bedded skeletal grainstone facies (Fig. 15A). Following the southward progradation trend, the tabular cross-bedded skeletal

grainstone facies is thickest at the Raghbah section and progressively thins towards Wadi Laban section before changing into the laterally equivalent facies downdip.

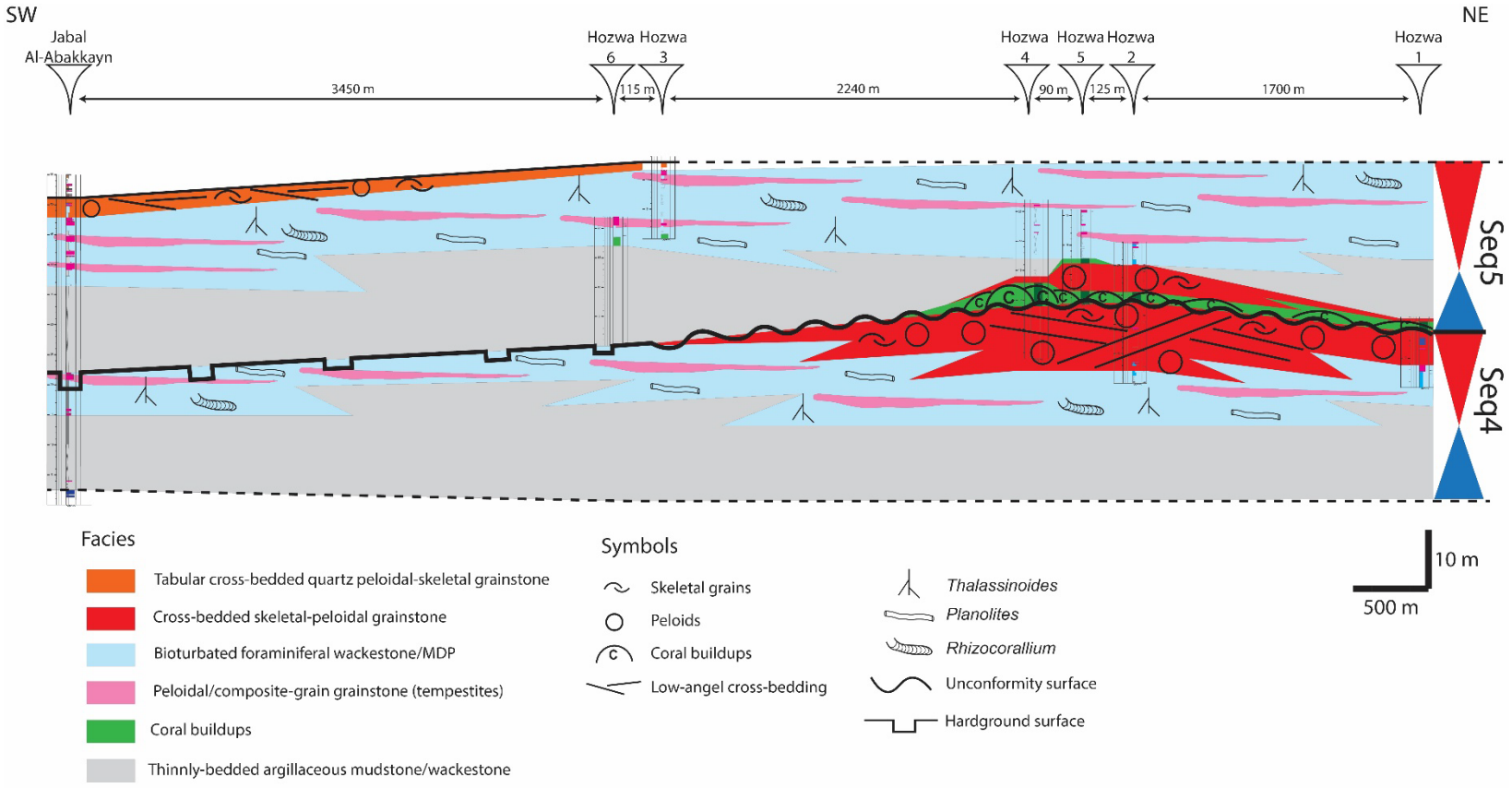

Fig. 16. Detailed stratigraphic framework of the Hanifa composite sequences 4 and 5 in the Hozwa area showing a rapid lateral facies change over a short distance between Jabal Al-Abakkayn and Hozwa. The unconformity surface is marked by karsting and is equivalent to a hardground surface at the Jabal Al-Abakkayn section. The argillaceous limestone pinches out against the coral buildups.

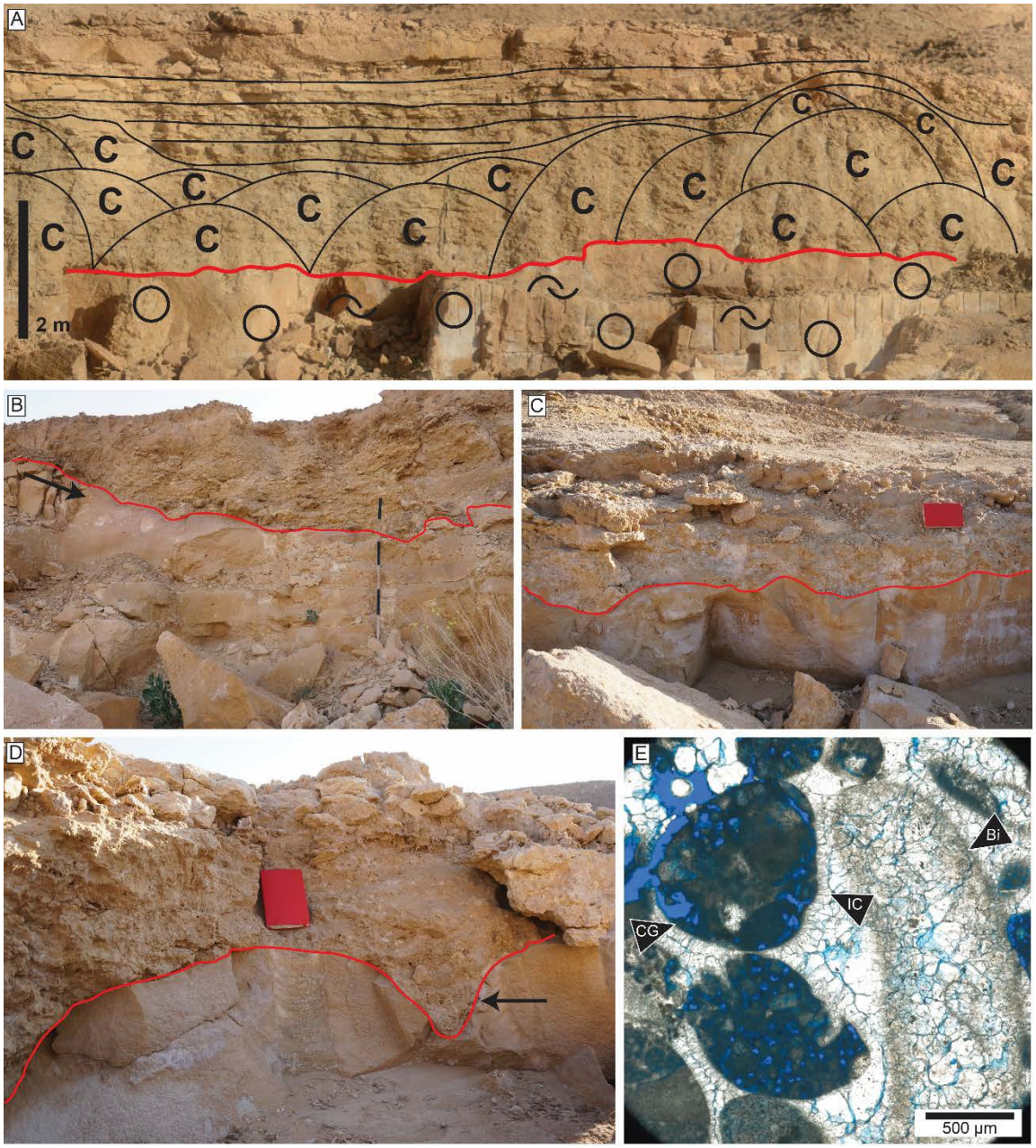

Fig. 17

Fig. 17. (**A**) The top of the cross-bedded skeletal-peloidal grainstone facies in Hozwa shows an erosional relief [red line] that is overlain by coral buildups [circles = peloids; shell symbols = skeletal grains]. (**B**) The erosional relief is recognized with a reddened surface [black arrow] [staff intervals = 20 cm]. (**C**) Field image showing the erosional surface [red line] at a smaller scale [notebook = 21 cm]. (**D**) A solution pipe [black arrow] over the peloidal grainstones demonstrating karstification associated with the exposure [notebook = 21 cm]. (**E**) Photomicrograph under plane-polarized light showing leached composite grains [CG] and bivalve fragment [Bi] with an isopacheous cement [IC]. The effect of exposure is illustrated at the micro-scale by extensive cementation and later dissolution, which resulted in the development of inter- and intraparticle porosities.

The sequence boundary of Seq5, equivalent to the top of the Hanifa Formation, is defined by a prominent facies offset. This is recognized by the change from the skeletal, stromatoporoid-coral, and oncolitic facies of the Hanifa to the interbedded echinoderm-brachiopod and tempestite facies of the basal Jubaila Formation (Figs. 14 and 18). At the Huraymila section in the north, the lateral equivalent to the tempestite and brachiopod wackestone/mud-dominated packstone facies are coral buildups that extend to the Raghbah section. Although the exposure at Raghbah ends at the top of the Hanifa, remnant fragments of corals are observed at the top suggesting the coral facies was laterally continuous from Huraymila section but was eroded with the current relief. Furthermore, the position of the coral buildups in the north relative to those in Seq5 indicates a retrogradational pattern associated with the Jubaila transgression. During this transgression, tempestites were frequent and widespread, indicating that the Arabian Shelf was a storm-dominated carbonate shelf (Fig. 18), which is a similar conclusion made by El-Asmar et al. (2015).

Overall, the stratigraphic framework of the Hanifa Formation shows the five composite sequences are superimposed into one second-order sequence. This sequence could be divided into two intervals, transgressive and regressive, that can correspond to the division of Vaslet et al. (1983; Fig. 2). Based on their subdivision, Hawtah Member is equivalent to the lower three composite sequences of the Hanifa Formation and Ulayyah is equivalent to the upper two sequences. However, a better assignment of the two members

is to relate them to the depositional system tracts of the Hanifa (Fig. 14). In this case, the Hawtah Member represents the transgressive system tract (TST) of the Hanifa and is dominated by the deposits of the distal lower shoreface and offshore environments. Conversely, the Ulayyah Member is equivalent to the highstand system tract (HST) of the Hanifa where the entire suite of the Hanifa facies is present. The turnaround between the TST and HST is marked by the widespread deposition of the thinly-bedded argillaceous mudstone/wackestone facies and absence of the coral buildups. This surface corresponds to the maximum flooding surface of the Hanifa Formation that occurs within Seq3. The use of this surface to define the Hawtah and Ulayyah Members could potentially be used to define them in the subsurface. Based on the Hanifa facies spectrum observed in the Ulayyah Member, the spatial relationships between facies were deciphered and allowed the construction of the Hanifa depositional model.

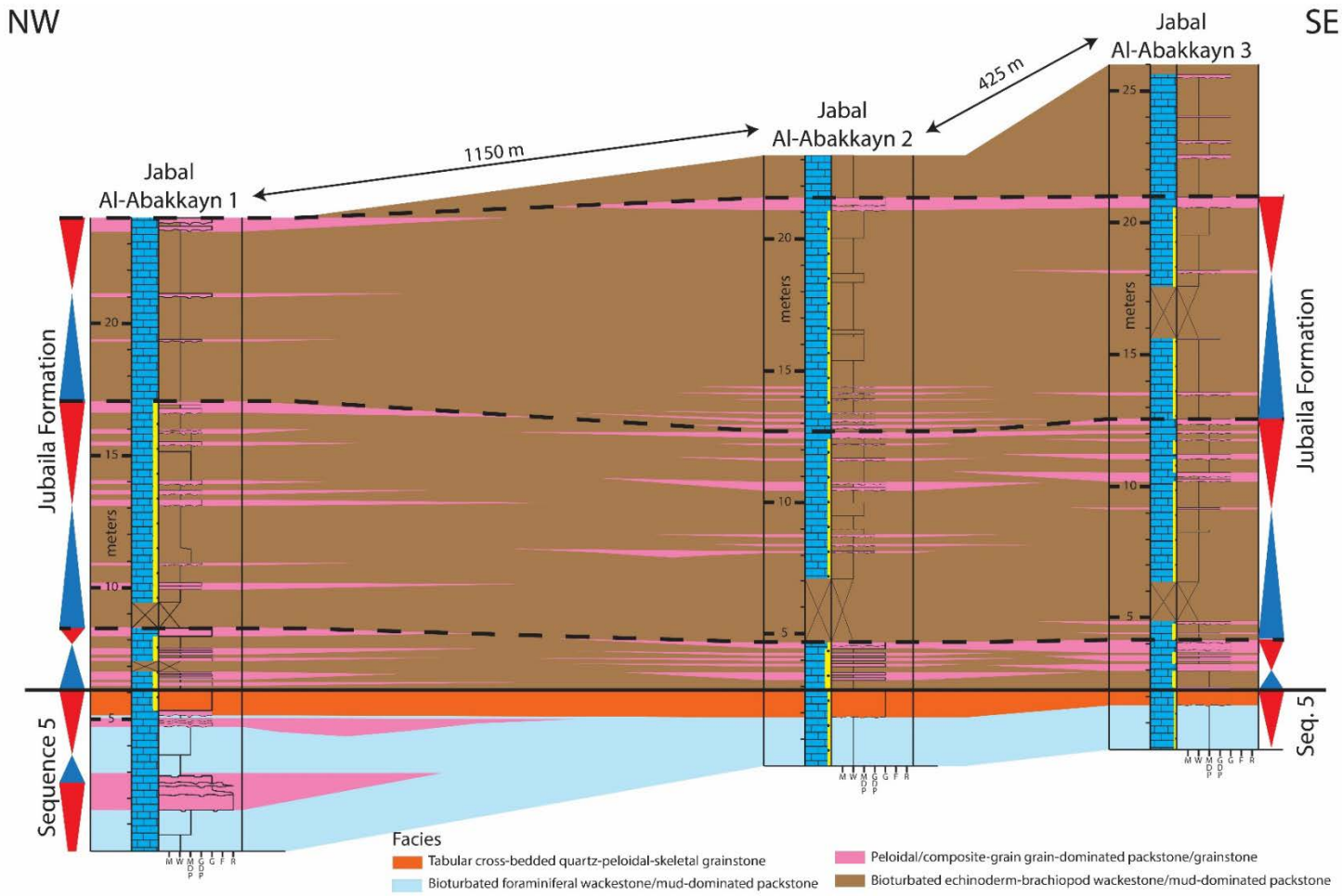

Fig. 18. Correlation between Jabal Al-Abakkayn measured sections showing the transition from the upper shoreface facies, cross-bedded peloidal-skeletal grainstone, of the Hanifa Formation to a storm-dominated shelf during the Jubaila Formation deposition

DEPOSITIONAL MODEL OF THE HANIFA FORMATION

The stratigraphic framework of the Hanifa Formation illustrates a two-dimensional facies distribution in time and space, thus allowing a depositional model to be constructed. The most complete representation of the depositional model comes from the HST of the Hanifa. Given the facies associations observed from the HST, a foreshore-shoreface-offshore model in a ramp profile is proposed (Fig. 19). The model shows a high-energy shoreline during the Hanifa deposition, represented by the foreshore and upper shoreface deposits. These include the cross-bedded peloidal grainstones of Hozwa as a local offshore island. The location of the shoal is assumed to be controlled by a local topographic high on the basis of the rapid lateral facies change observed (Figs. 14 and 16). The shoal complex would probably have been oriented NE-SW, parallel to the prevailing wind direction (Fig. 1), but the detailed three-dimensional mapping required to demonstrate this has yet to be done. In addition, if other shoal bodies existed in the same manner, they would not have formed energy barriers for the main shoreline further updip, which is marked by foreshore deposits. Foreshore deposits are not observed in the study area, but they are extrapolated to exist north of the study area based on the northward shallowing-upward trend observed.

Downdip on the depositional model, the relationship between the stromatoporoid-coral and oncolitic facies is demonstrated (Fig. 19). The coral bioherms were deposited in a moderately high-energy environment where they formed disconnected bodies parallel to depositional strike, whereas the coral biostromes were deposited in a low-energy environment but were more laterally continuous. Within the peripheral area of the corals, the oncoids formed mainly around the buildups and filling the lows between them. This relationship is supported by field observations such as the growth of isolated coral heads and presence of coral fragments within the oncolites (Fig. 8).

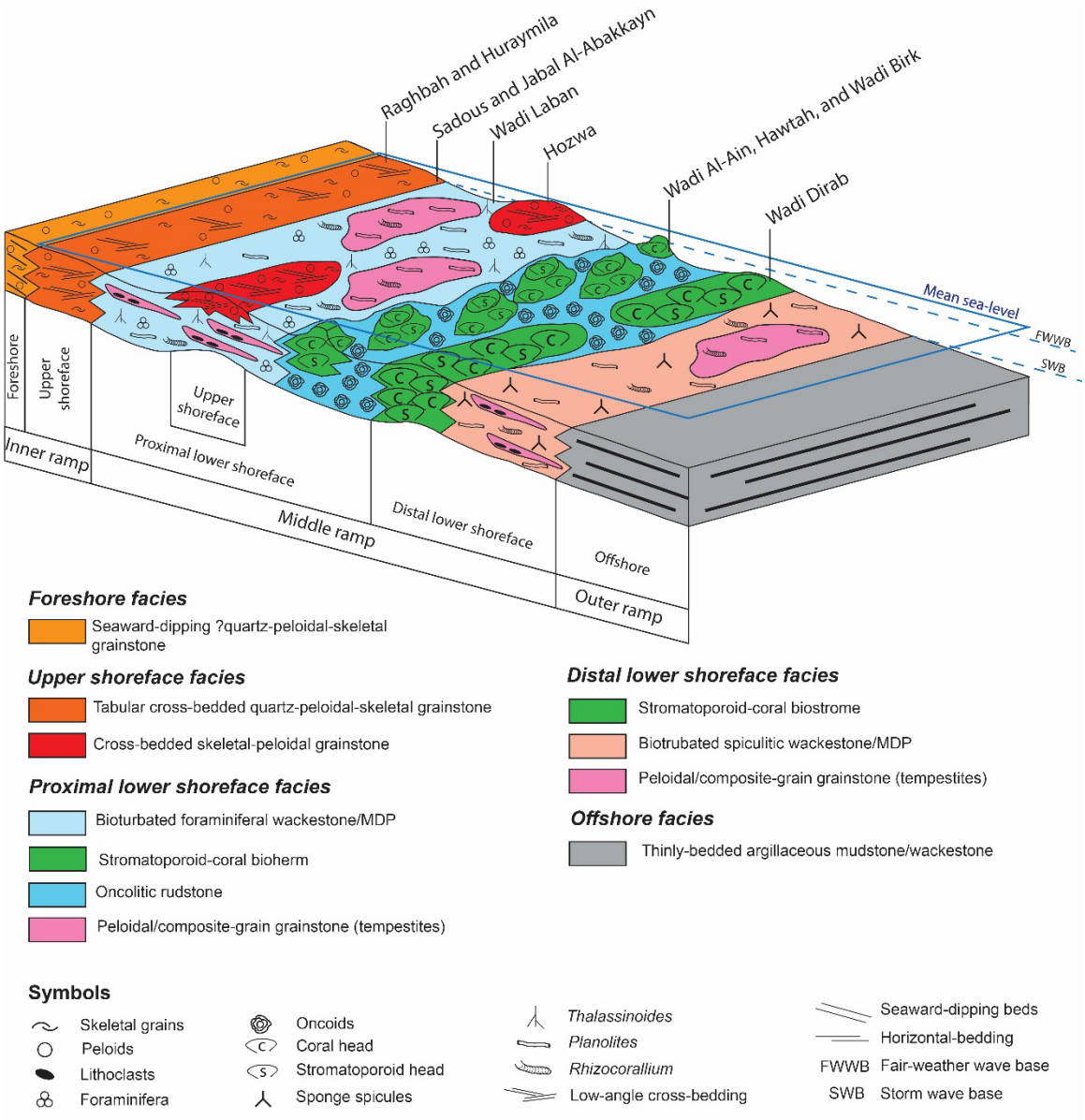

Fig. 19. Idealized depositional model for the Hanifa Formation (not to scale) showing the depositional setting as a gently sloping ramp that was episodically affected by storm events.

DISCUSSION

STUDY FINDINGS FROM THE PERSPECTIVE OF PREVIOUS WORKS

Accommodation during the time of the Hanifa deposition was greater in the southern part of the exposure belt, which is evident by the southward thickening of the Hanifa Formation. This trend was also noted by Enay et al. (1987). The greater accommodation resulted in the preservation of five composite sequences in the south compared to four composite sequences in the north. The additional sequence suggests that the initial Hanifa transgression over the exposure belt started from the south and onlapped over the top of the Tuwaiq Mountain Limestone. It also suggests the transgression was probably gradual and not widespread, which is also interpreted from the retrogradation of the coral buildups. Furthermore, the progradation trend during the Hanifa highstand was to the south as is evident by the coral buildups and upper shoreface deposits. From this, it could be concluded that the persistent accommodation in the south suggests a possible extension of the Arabian or Rub' Al-Khali intrashelf basins to the south and southwest of the exposure belt.

Le Nindre et al. (1990) indicated the Hanifa Formation composes five depositional sequences that correspond to the supercycle LZA-4 of Haq et al. (1988). Their interpretation was based on biostratigraphic and lithostratigraphic data, however, they did not illustrate how these sequences would be recognized in the outcrop. As a result, it is difficult to assess the correspondence between the results herein and their interpretation. In addition, Le Nindre et al.'s (1990) division of the Hanifa into five depositional sequences does not hold true everywhere at the exposure belt as illustrated in this study (Figs. 14 and 20). This illustrates the importance of 2-dimensional, and if possible 3-dimensional, analysis on a large regional scale for establishing a stratigraphic framework in such a broad carbonate platform. A 1-dimensional analysis would not yield the same results, as there is not a single section representative of all Hanifa facies. This is related to lateral facies changes occurring gradually over long distances or to the orientation of the exposure belt being oblique to the depositional strike and dip. With such an orientation, it is hard to assess the dimensionality of the facies belts and how far apart are they from one another.

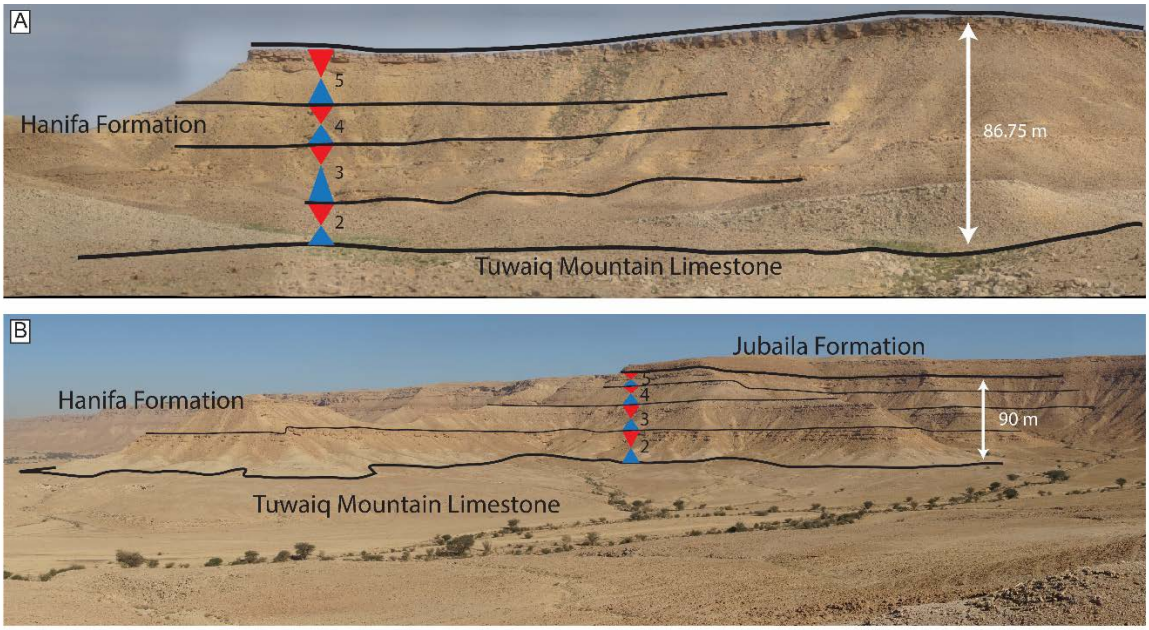

Fig. 20. (**A**) The Hanifa exposure at Raghbah showing the four Hanifa sequences in the northern part of the study area. The sequences are associated with resistive beds corresponding to the grainstone and bioherm facies that can be traced over relatively long distances. (**B**) The upper four sequences of the Hanifa Formation at Wadi Dirab are commonly associated with resistive beds corresponding to the grainstone, oncolite, and biostrome facies.

Despite the localized unconformity surface at Hozwa, the pick for the Hanifa top at Seq5 is regionally consistent. It follows an overall shallowing-upward trend that is defined by the tabular cross-bedded peloidal grainstones in the north and by the oncolites and coral buildups in the south (Fig. 21). The defined Hanifa top is generally consistent with the interpretation of Manivit et al. (1985) and Vaslet et al. (1983). Nevertheless, the Hanifa top in the area of Wadi Dirab and Wadi Laban interpreted by Vaslet et al. (1991) is effectively placed within the tempestites of basal Jubaila Formation. Based on the Hanifa stratigraphic framework proposed here, the contact with the Jubaila Formation is strikingly sharp and denotes the shift into a storm-dominated shelf. Because of this observation, the top of the Hanifa at Wadi Dirab is placed on top of the coral biostromes (Fig. 21).

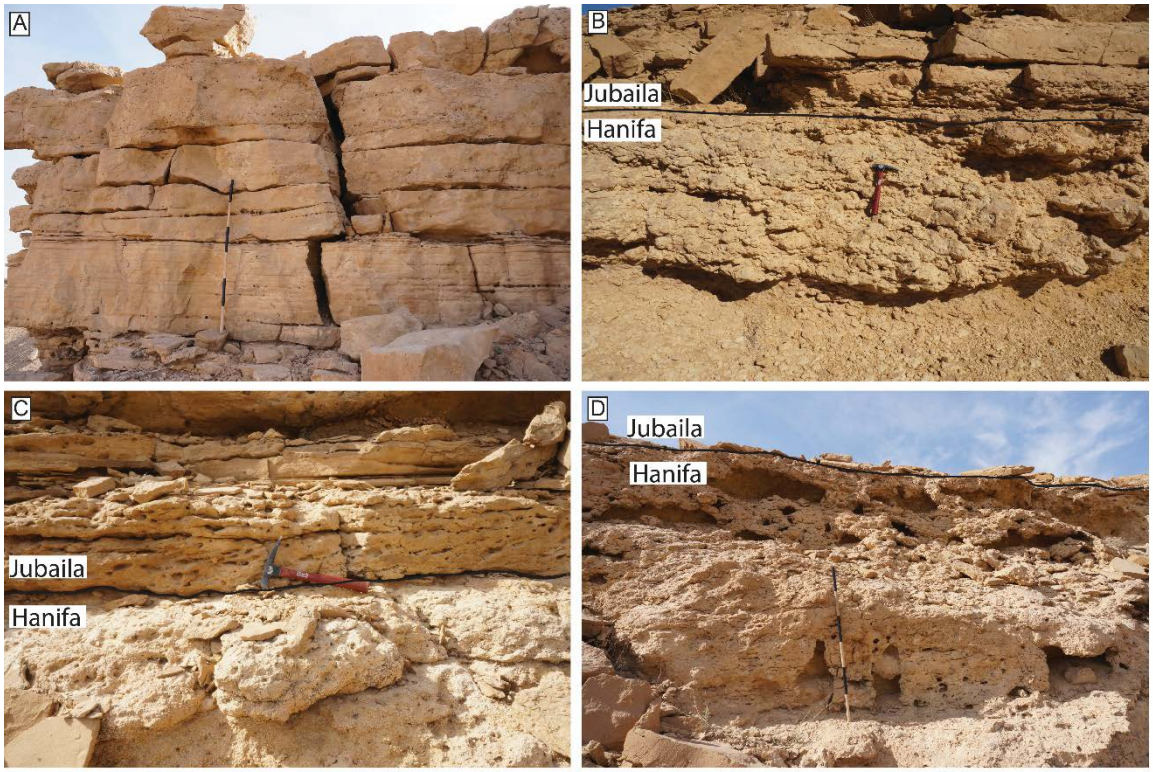

Fig. 21. (**A**) The top of the Hanifa Formation at Raghbah is marked by a prominent bench formed by the cross-bedded peloidal-skeletal grainstone facies [staff intervals = 20 cm]. (**B**) At Wadi Dirab, the top of the Hanifa is defined by a sharp surface between a coral biostrome below and storm event beds above [hammer = 30 cm]. (**C and D**) At Wadi Al-Ain, the contact with the Jubaila Formation is marked by either oncolitic rudstone (**C**) or coral buildups (**D**) of the Hanifa below and the tempestites of the Jubaila above [hammer = 30 cm; staff intervals = 20 cm].

Evidence for the paleoshoreline during the Hanifa time is indicated by the upper shoreface facies, the tabular cross-bedded quartz-peloidal-skeletal grainstone facies (Figs. 5 and 22). The presence of angular to subangular quartz grains within this facies supports the proximity to the shoreline. Based on facies associations described here, the Hanifa Formation had a high-energy shoreline. Although Moshrif's (1984) depositional model for the Hanifa Formation represents a ramp depositional setting as this study shows, it indicates the presence of tidal flats based on gypsum precipitates, which suggests a low-energy

shoreline. However, very thin gypsum layers were observed sporadically in the outcrop as recent diagenetic residuals that do not occur in association with a particular facies. Hughes et al. (2008) proposed a rimmed-platform as a depositional model for the Hanifa Formation, which was based mostly on paleontological data with minimal sedimentological analysis. Their interpretation appears to be unrealistic given the facies associations observed and the paleogeographic location from the actual shelf margin (Fig. 1). Therefore, it is very crucial to conduct a detailed sedimentological study to help proposing a realistic depositional model.

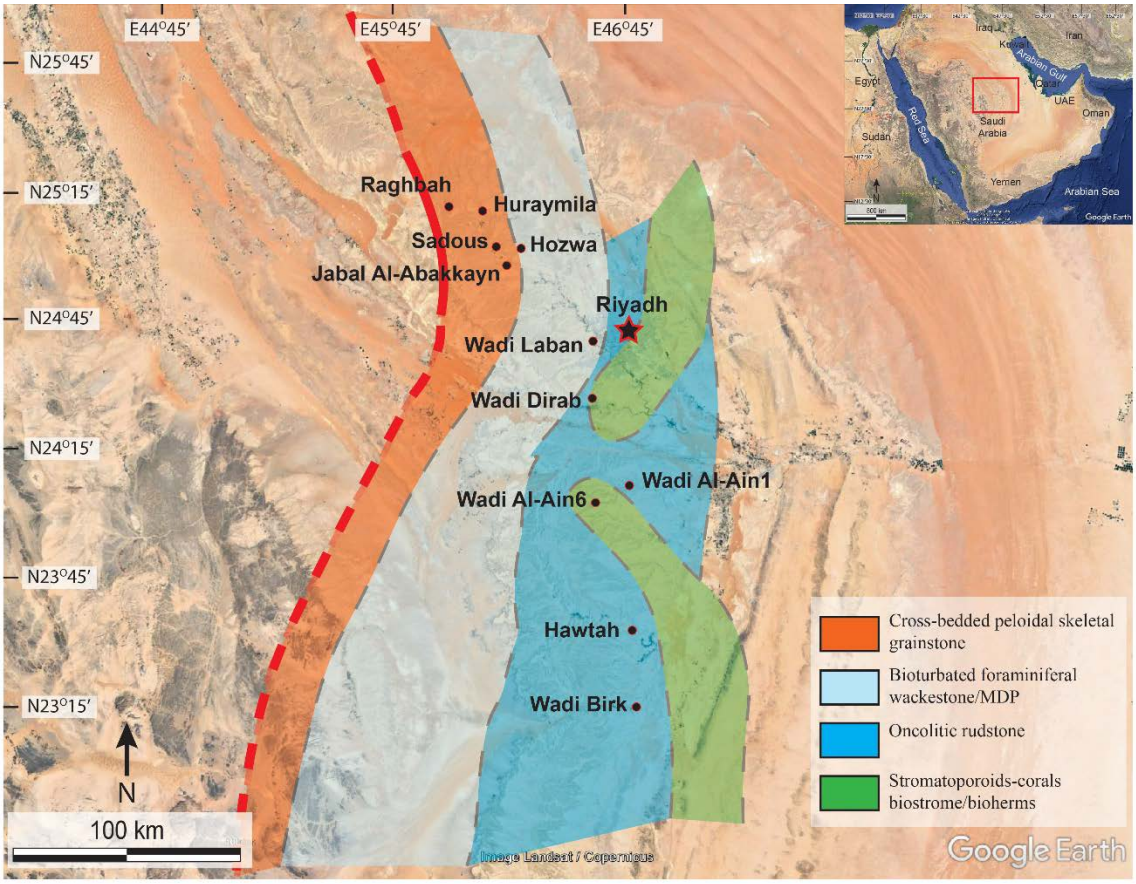

Fig. 22. The interpreted paleoshoreline (red dashed-line) during the HST of Hanifa is based on the presence of high-energy, shallow-water deposits in conduction with detrital quartz grains.

COMPARISON WITH SIMILAR JURASSIC SYSTEMS

Given the maximum duration of the Hanifa deposition of 5.5 Ma (Hughes et al., 2008), the accumulation rate for the Hanifa is 26 m/million year (my). This is such a slow rate in comparison with other Jurassic systems, but it is not unusual. Bosscher and Schlager (1993) calculated the accumulation rate for some Jurassic units in the literature to be in the range 18.2 – 166.7 m/my. According to their analysis, rates above 25 m/my over a period of 1 – 10 Ma are associated with relative sea-level rise driven rather by subsidence more than eustasy. Sharland et al. (2001) indicated the transgression event at the base of the Hanifa coincided with the development of intrashelf basins, as noted by Droste (1990). However, the flooding event seems to be eustatically controlled rather than controlled by subsidence. Le Nindre et al. (2003) illustrated a period of minimal subsidence during Hanifa time, which is also evident from other parts of the Arabian Plate. In Yemen, for instance, Shuqra Shale of Oxfordian – Kimmeridgian age was deposited as a result of continued transgression over the Central Ayad High. The shale, as mapped by Brannan et al. (1999), does not show thickening over the graben of the Central Ayad High, which indicates the bounding fault was not active during the shale deposition and supporting a minimal effect of subsidence.

In the Swiss Jura carbonate platform, Jank et al. (2006) defined five third-order sequences for the Late Oxfordian – Late Kimmeridgian Reuchenette Formation. These sequences are superimposed into two second-order sequences compared to one sequence for the Hanifa Formation as recognized in this study. Jank et al.'s (2006) five depositional sequences were driven by eustatic fluctuations as they were correlatable to equivalent Boreal realm sequences. The similar trend was also observed by Colombié and Rameil (2007) where they illustrated, with supporting ammonite zonation data, the correlation of third-order depositional sequences between the Tethyan and Boreal realms. This supports the interpretation of global eustatic fluctuations controlling relative sea-level changes for the Hanifa depositional sequences.

Similarly, Olivier et al. (2015) identified six stages for the development of the French Jura carbonate platform during Late Oxfordian – Early Kimmeridgian. These stages

correspond to seven depositional sequences where the sixth stage consists of two sequences. The unique characteristic of the last stage is that the platform evolved into a flat-topped shelf in response to a long-term transgressive event and change in climate. Based on Olivier et al. (2015) analysis, carbonate production was low due to high influx of terrigenous materials, which was attributed to a semi-arid climate with seasonal humidity. This climatic change could explain the sharp change into a storm-dominated shelf with the transgression of the Jubaila Formation (Figs. 14 and 18). It may also mark the change into an arid climate for the subsequent evaporite – carbonate sequences of the Arab Formation in the Late Kimmeridgian – Tithonian (Fig. 2). Furthermore, terrigenous input is evident by the presence of quartz grains within the storm beds and bioturbated brachiopod wackestone facies of basal Jubaila Formation (Figs. 10I and 11D).

The climatic signal appears to be consistent along the Tethys during the Kimmeridgian. Shallow-marine carbonate platforms in Spain (Molina et al., 1997; Bádenas and Aurell, 2001; Colombié et al., 2014) and France (Seguret et al., 2001) were storm-dominated shelves. The trend where quartz grains observed in the HST of the Hanifa Formation within the cross-bedded skeletal grainstone (Figs. 5D and 5E) and in the TST of the Jubaila Formation within the storm beds (Fig. 10I) was also noted by Bádenas and Aurell (2001). They demonstrated that quartz grains were more abundant within cross-bedded oolitic grainstones during HST and more abundant within distal tempestites of TST. This further supports the interpretation of the paleoshoreline proximity to the cross-bedded skeletal grainstone during HST of the Hanifa Formation.

IMPLICATIONS FOR HYDROCARBON EXPLORATION AND DEVELOPMENT

The Hozwa peloidal grainstone shoal demonstrates a rapid lateral facies change over a short distance under certain conditions indicating an exception to the rule that generally rapid facies are not common in this depositional setting. The location of the shoal might suggest a preexisting topographic high that controlled their deposition. The unconformity surface that is only recognized at Hozwa supports the interpretation in which the topographic relief aided the development of the erosional and karst surfaces.

Furthermore, this antecedent relief is evident by the nucleation of coral buildups with Seq5 transgression on top of the peloidal grainstones. This behavior of buildup growth in association with transgression and topographic highs has been documented by Friebe (1993) and Krause Jr. and Meyer (2004). If the topographic high at Hozwa was a persistent structure through time, there might be a potential for a hydrocarbon structural-trap for the Paleozoic petroleum system in Central Arabia. Furthermore, the Hozwa area is a significant site as it exposes Hanifa Reservoir facies, peloidal grainstone and coral bioherms (McGuire et al., 1993), which can be used as an analog for subsurface studies. The maximum flooding surface (MFS) of the Hanifa identified in this study corresponds to the MFS J50 of Sharland et al. (2001), which coincided with the deposition of organic-rich source rock in the intrashelf basins. Correlation with Sharland et al.'s (2001) MFS J50, indicates the argillaceous mudstone/wackestone facies is laterally equivalent to organic-rich source rocks. Therefore, the recognized basin to the south and southwest of the exposure belt is a potential area for unconventional plays, as has been suggested by Hughes et al. (2008).

The Hanifa stratigraphic framework presented here demonstrates how possible reservoir facies are distributed in a depositional profile. The lateral and vertical facies relationships observed in the field can be used as analogs for constructing reservoir frameworks in the subsurface. Moreover, the Hanifa depositional model provides a predictive tool for exploration of new Hanifa targets. For instance, the stromatoporoid-coral facies is a reservoir facies in Berri Field that is observed at the upper part of the Hanifa Formation (McGuire et al., 1993). Based on the stratigraphic framework, this facies exists in the lower part of the formation (Fig. 14), which receives less attention when exploring for a conventional hydrocarbon target within the Hanifa Formation.

CONCLUSIONS

The sequence stratigraphic framework established in this study provides the first regional understanding of the Hanifa exposure along the Tuwaiq Escarpment in Central Arabia. The study demonstrates the spatial and temporal distribution of eight identified facies in the Hanifa Formation and presents the first evidence for the paleoshoreline during Hanifa time.

On the basis of this study, the Hanifa Formation displays an overall thickening to the south of the Tuwaiq Escarpment. This indicates the possible extension of the Arabian or Rub' Al-Khali intrashelf basins into the southern end of the exposure belt, which created greater accommodation in the south. This trend is represented by the differential development of depositional sequences across the 260 km distance of the study area. In the north, the Hanifa Formation is divided into four composite sequences, whereas in the south five composite sequences are identified given the greater accommodation that was available. The major criteria for recognizing these sequences were sharp facies offset, facies proportions, and exposure-related erosion. The erosional surface was only observed at Hozwa, where a skeletal-peloidal shoal complex developed. Its location was controlled by a topographic high at the time of deposition. Accordingly, the division of the Hanifa Formation into two members holds and corresponds to the two system tracts recognized. The lower member, Hawtah, represents the TST whereas Ulayyah corresponds to the HST. The maximum flooding surface of the Hanifa Formation lies within the third composite sequence (Seq3) and is characterized by an absence of coral buildups, and widespread deposition of thinly-bedded argillaceous mudstone/wackestone facies. Also, this surface marks the boundary between the two members. The development of these sequences was driven by eustatic fluctuations that can be correlated globally.

The sequence stratigraphic framework of the Hanifa Formation indicates a foreshore-shoreface-offshore depositional model where it shows the high-energy character of the shoreline under normal open-marine conditions. During the HST of the Hanifa, the paleoshoreline was to the north of the study area. The upper shoreface deposits (tabular cross-bedded quartz-peloidal-skeletal grainstones) mark the proximity to the shoreline,

whereas the skeletal-peloidal shoal at Hozwa represents a localized shoreline. Foreshore deposits are assumed to exist north of the study area on the basis of the northward shallowing-upward trend. This shallowing-upward trend interrupted by a sharp facies offset related to the transgression of the overlying Jubaila Formation marks the contact between the Hanifa and Jubaila Formations. On the basis of facies association of basal Jubaila, the Arabian Platform was a storm-dominated shelf during the Early Kimmeridgian. This drastic shift was caused by a change into a semi-arid climate and potentially towards an arid climate for the evaporite – carbonate sequences of the Arab Formation.

The vertical and lateral facies distribution provide outcrop analogs for the equivalent subsurface geology. Facies juxtaposition relationships can help in building reservoir models if similar facies existed in the subsurface. Furthermore, if the topographic high at Hozwa was a persistent structure through time, there might be a potential for a hydrocarbon structural-trap for the Paleozoic petroleum system. Also, the basinal area identified to the south and southwest of the study area might have a potential for unconventional plays.

APPENDIX

The appendix is intended to provide the detailed description of each measured section of the Hanifa Formation along the Tuwaiq Escarpment, excluding those provided by Abdullah Al-Mojel.

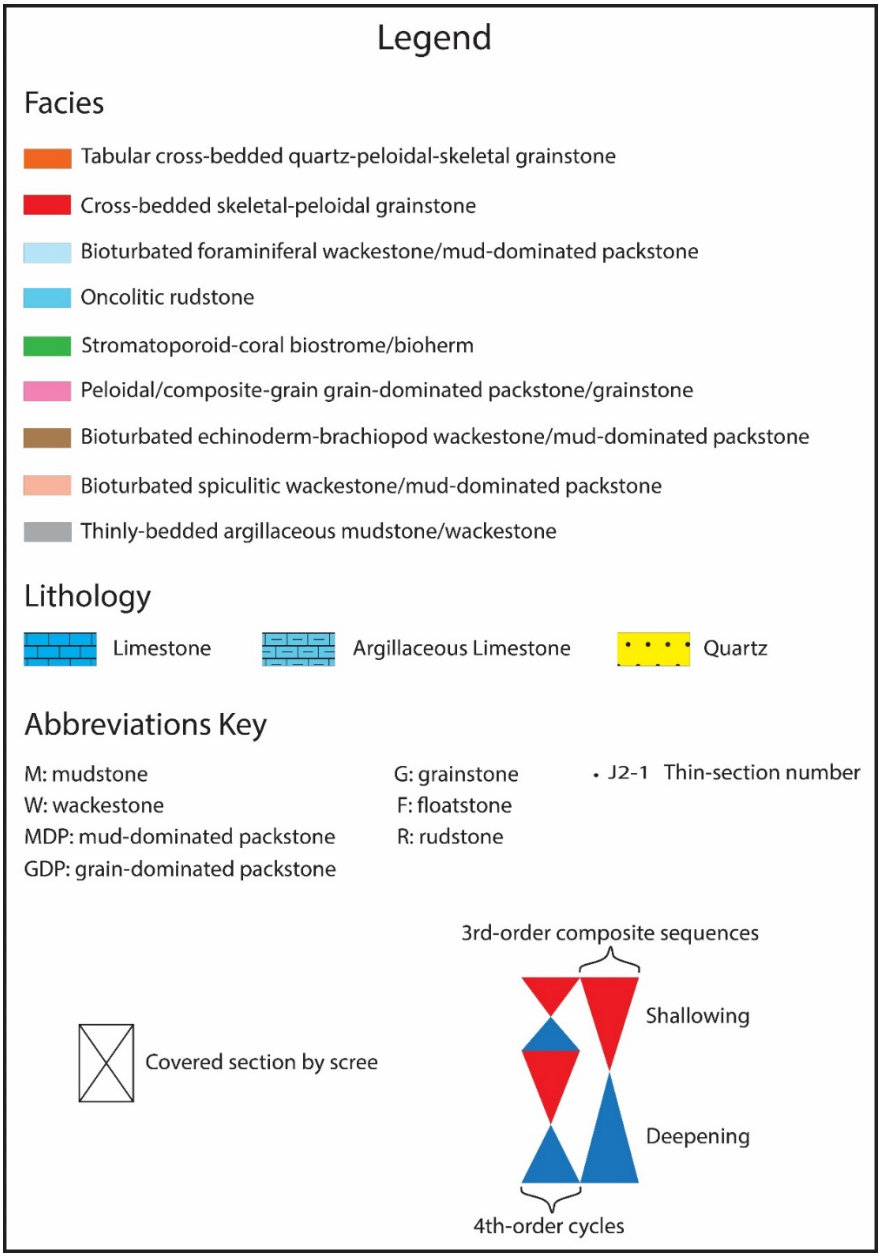

Raghbah measured section

from 25°13'6.00"N ; 45°57'25.00"E to 25°12'52.69"N ; 45°58'4.68"E

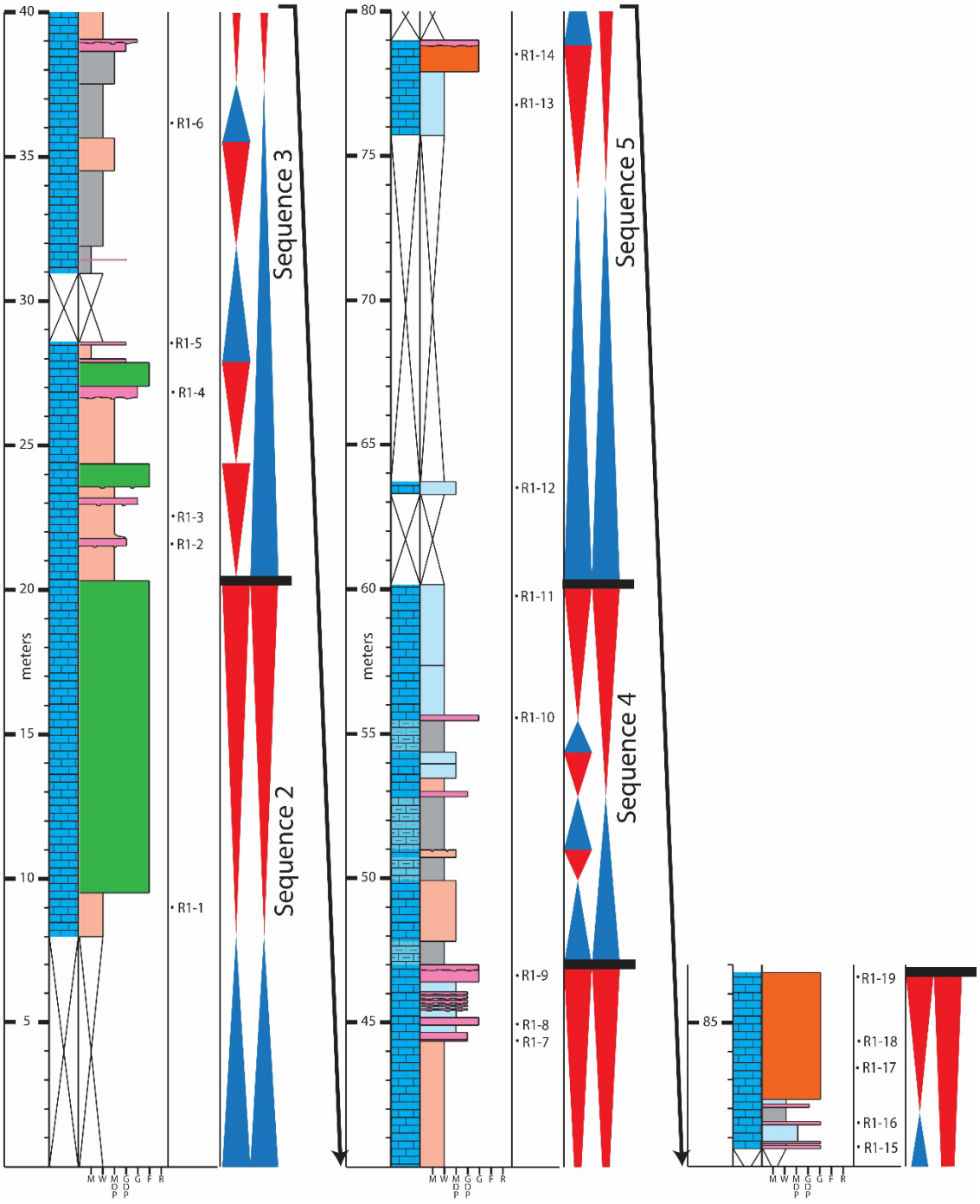

Huraymila measured section

@ 25°9'21.00"N ; 46° 6'38.00"E

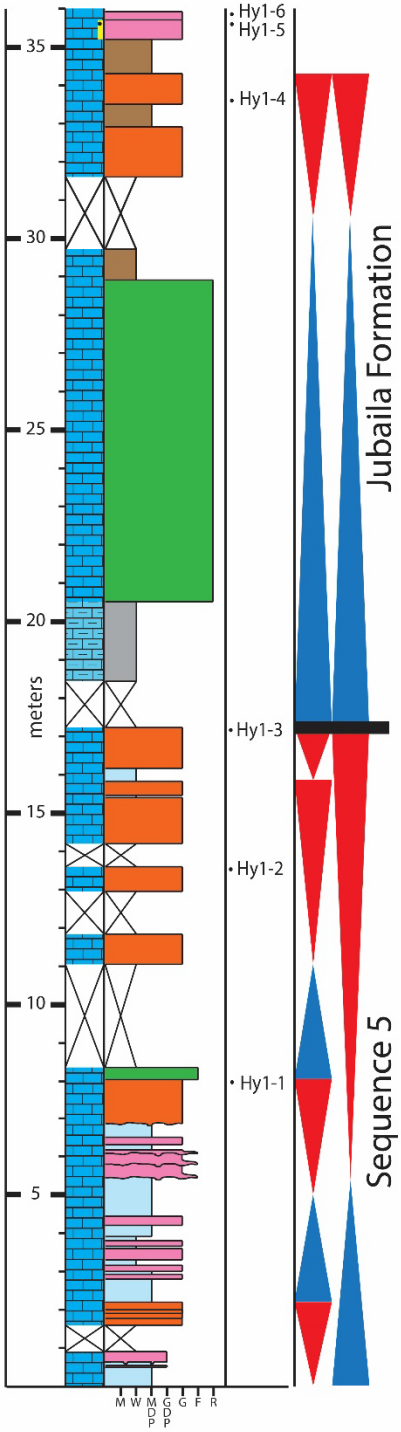

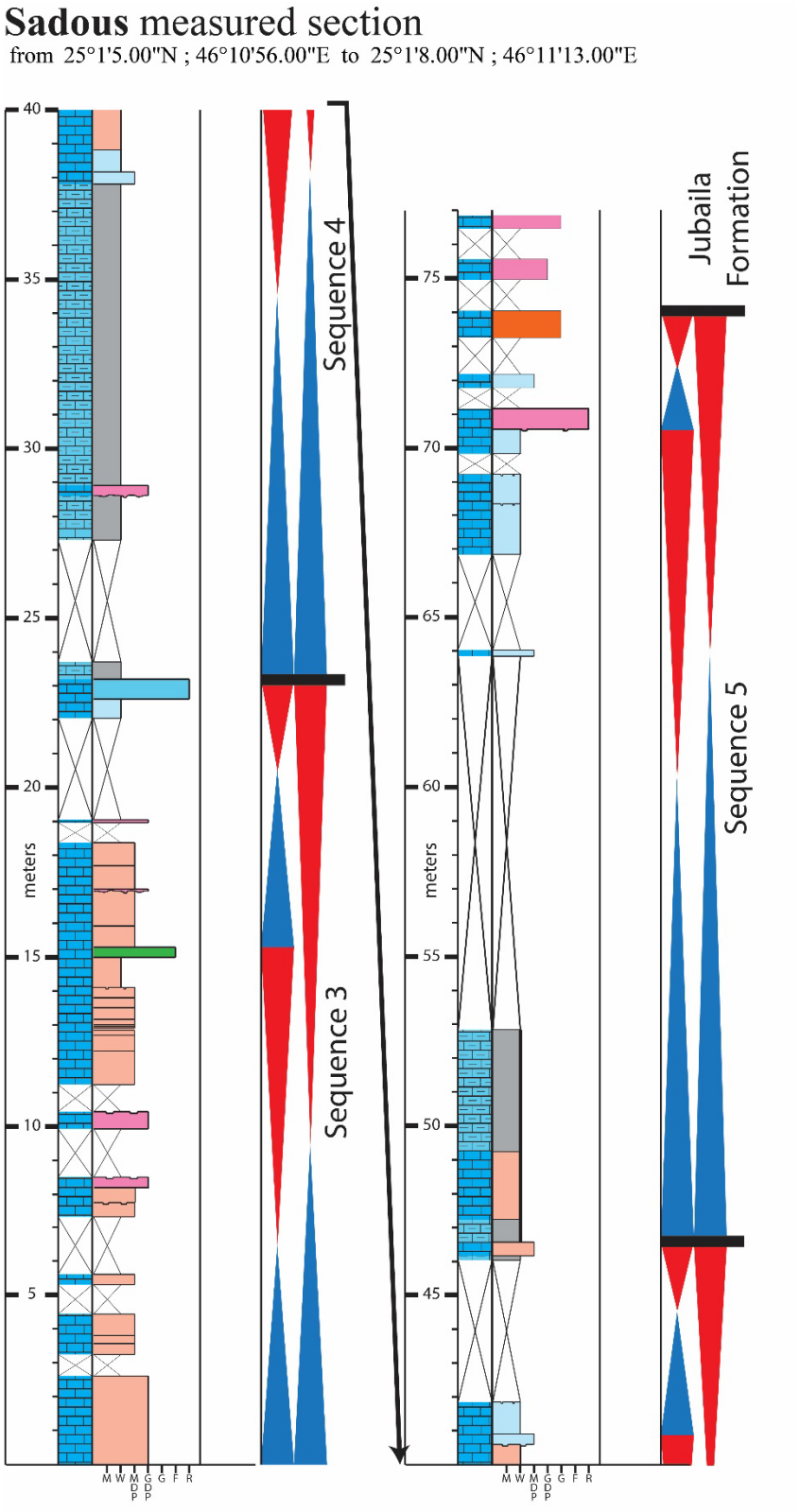
Sadous measured section
from 25°1'5.00"N ; 46°10'56.00"E to 25°1'8.00"N ; 46°11'13.00"E
meters
40
35
30
25
20
15
10
5
M W M G G F R
D D
P P
Sequence 4
Sequence 3
meters
75
70
65
60
55
50
45
M W M G G F R
D D
P P
Jubaila Formation
Sequence 5

Hozwa 1 measured section
@ 25°0'57.00"N ; 46°16'8.00"E

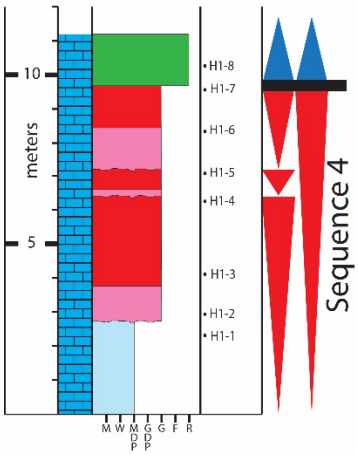

Hozwa 3 measured section
@ 24°59'28.98"N ; 46°14'18.20"E

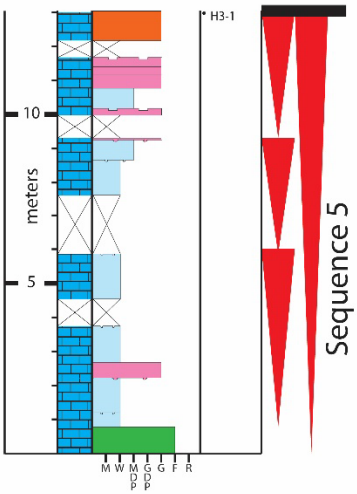

Hozwa 2 measured section
@ 25°0'15.10"N ; 46°15'27.75"E

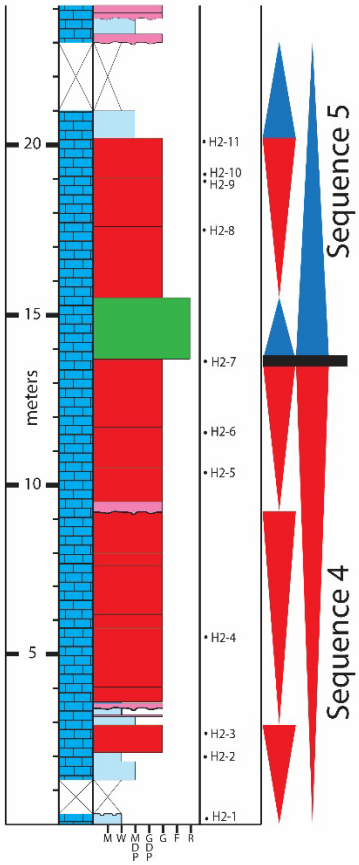

Hozwa 4 measured section
@ 25°0'9.41"N ; 46°15'24.15"E

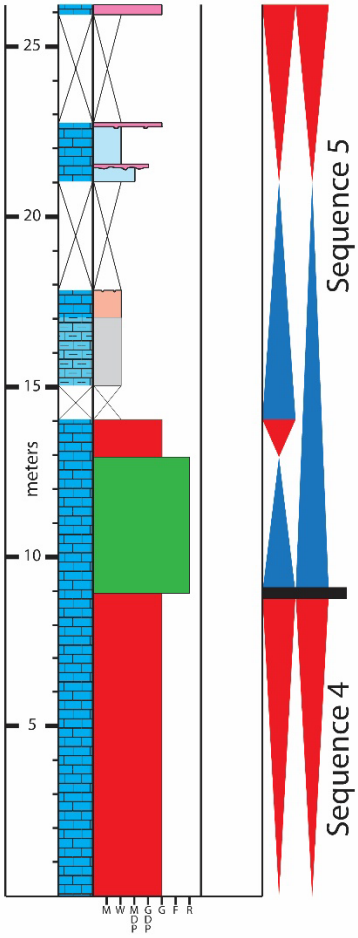

Hozwa 5 measured section
@ 25°0'11.00"N ; 46°15'27.00"E

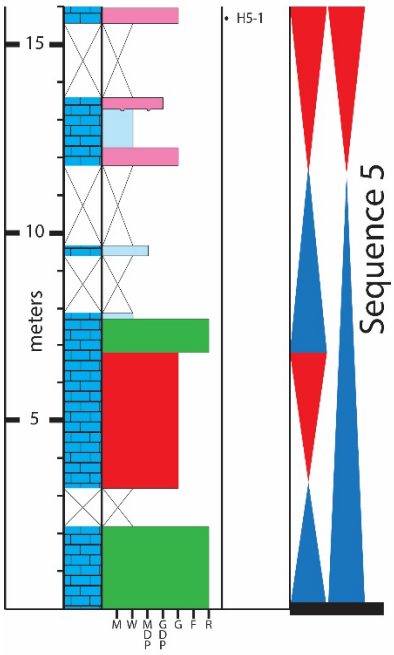

Hozwa 6 measured section
@ 24°59'28.00"N ; 46°14'14.00"E

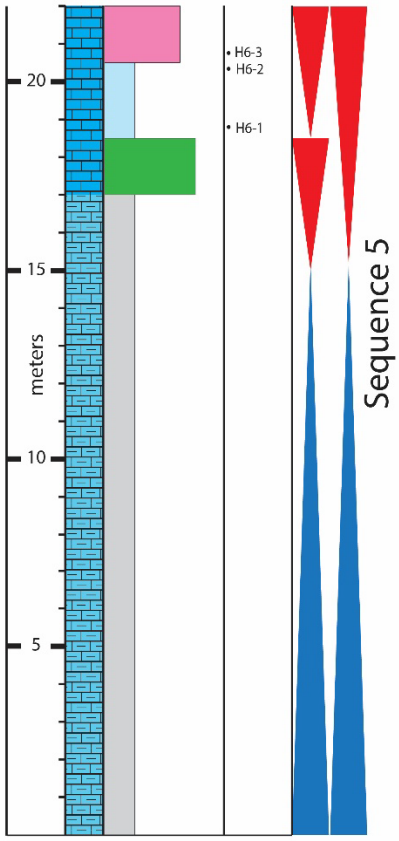

Jabal Al-Abakkayn 1 measured section

from 24°57'37.00"N ; 46°11'33.00"E to 24°57'59.00"N ; 46°13'27.00"E

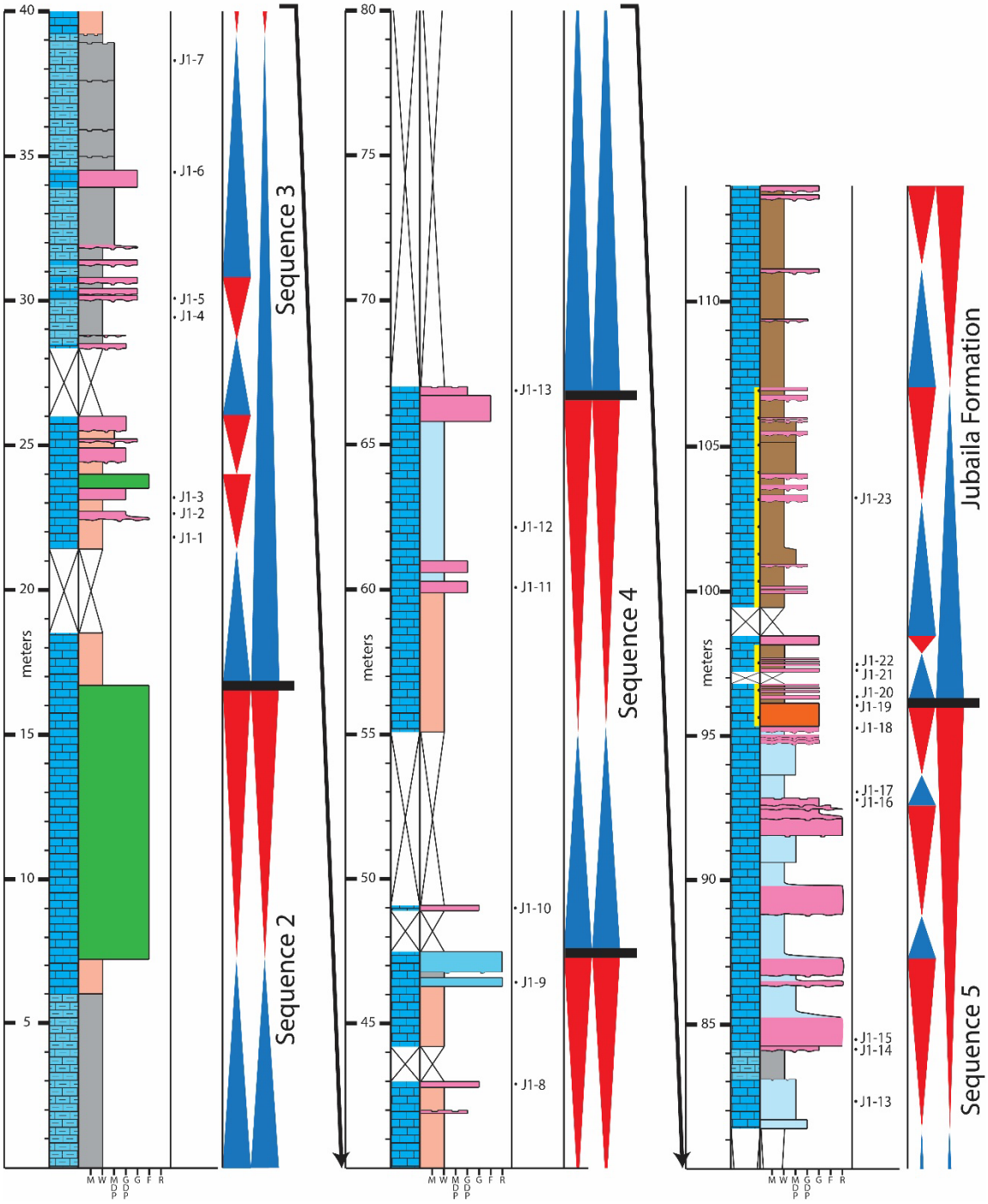

Jabal Al-Abakkayn 2 measured section
@ 24°57'38.00"N ; 46°14'9.00"E

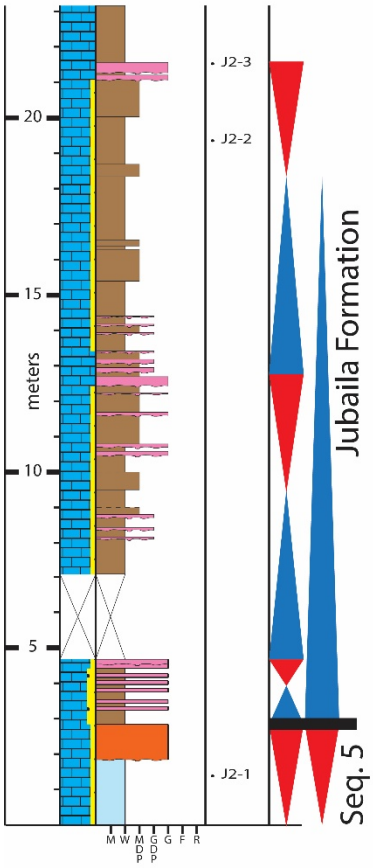

Jabal Al-Abakkayn 3 measured section
@ 24°57'27.00"N ; 46°14'18.00"E

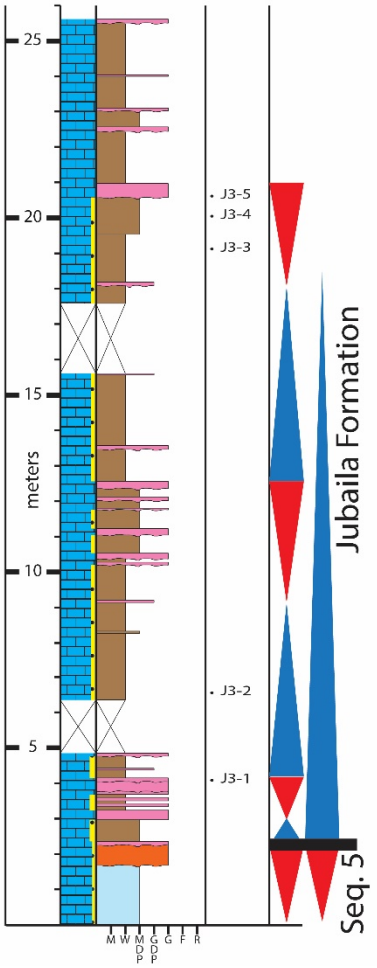

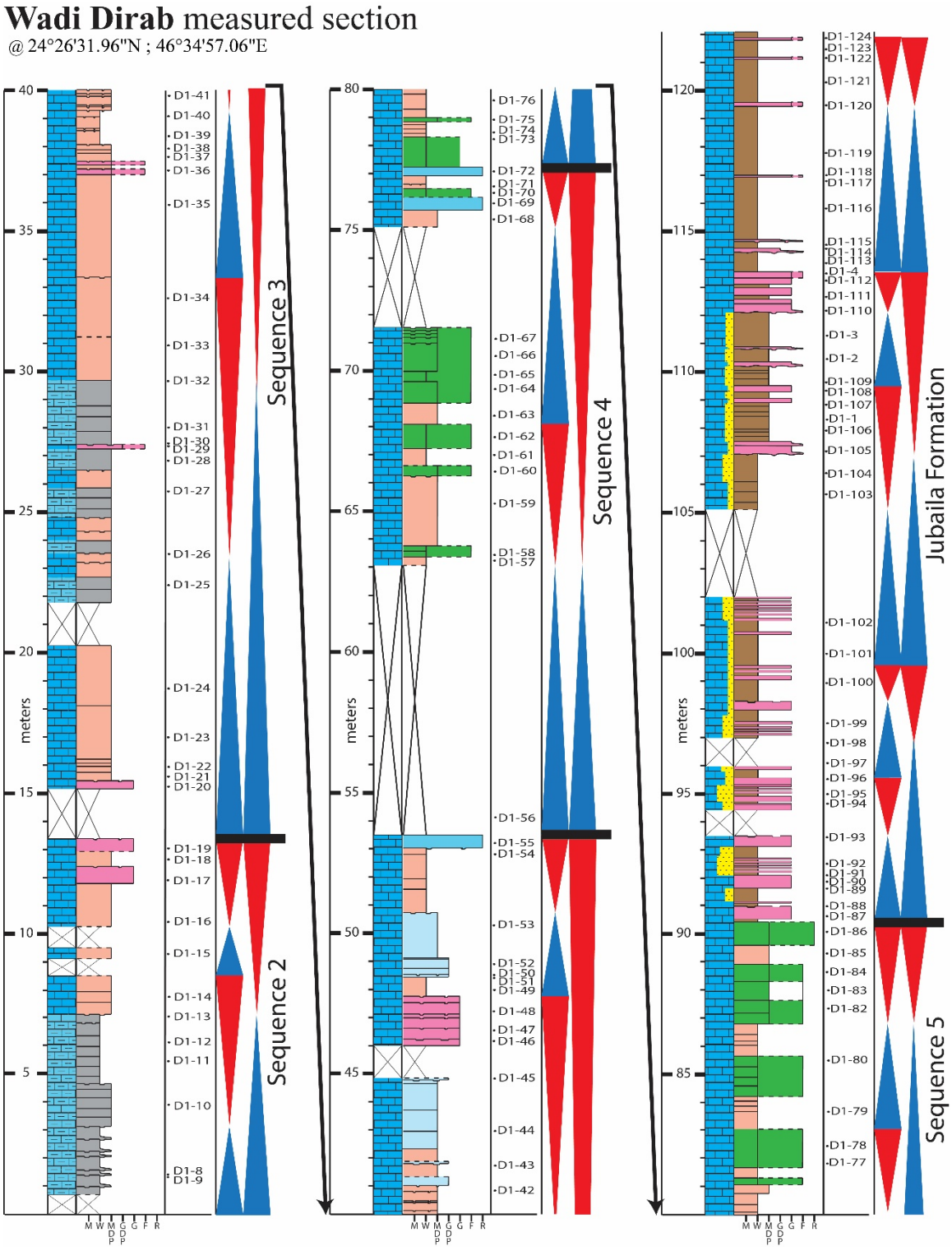
Wadi Dirab measured section
@ 24°26'31.96"N ; 46°34'57.06"E
meters
Sequence 2
Sequence 3
Sequence 4
Sequence 5
Jubaila Formation

Wadi Al-Ain 1 measured section

from 24°6'51.19"N ; 46°45'2.20"E to 24°6'48.29"N ; 46°45'5.18"E

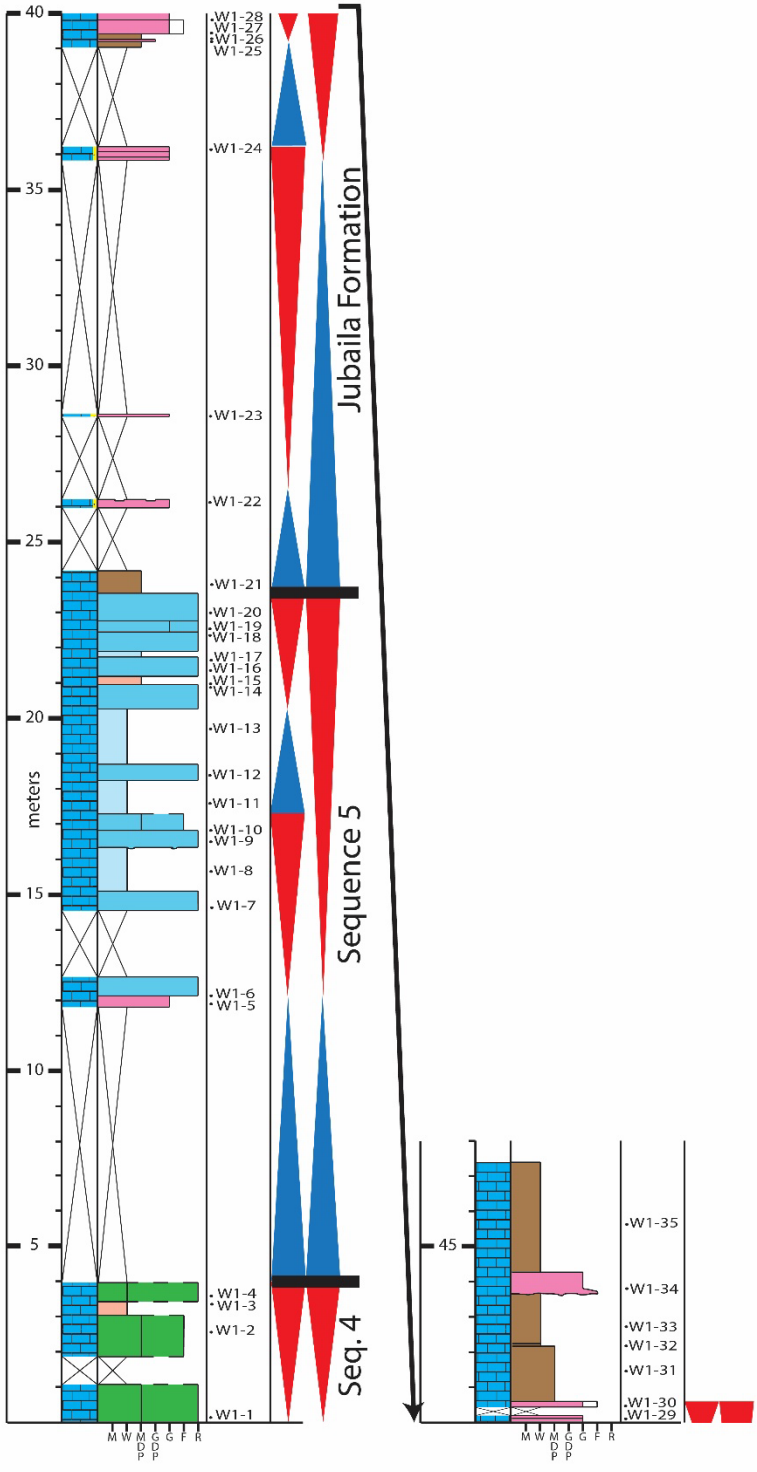

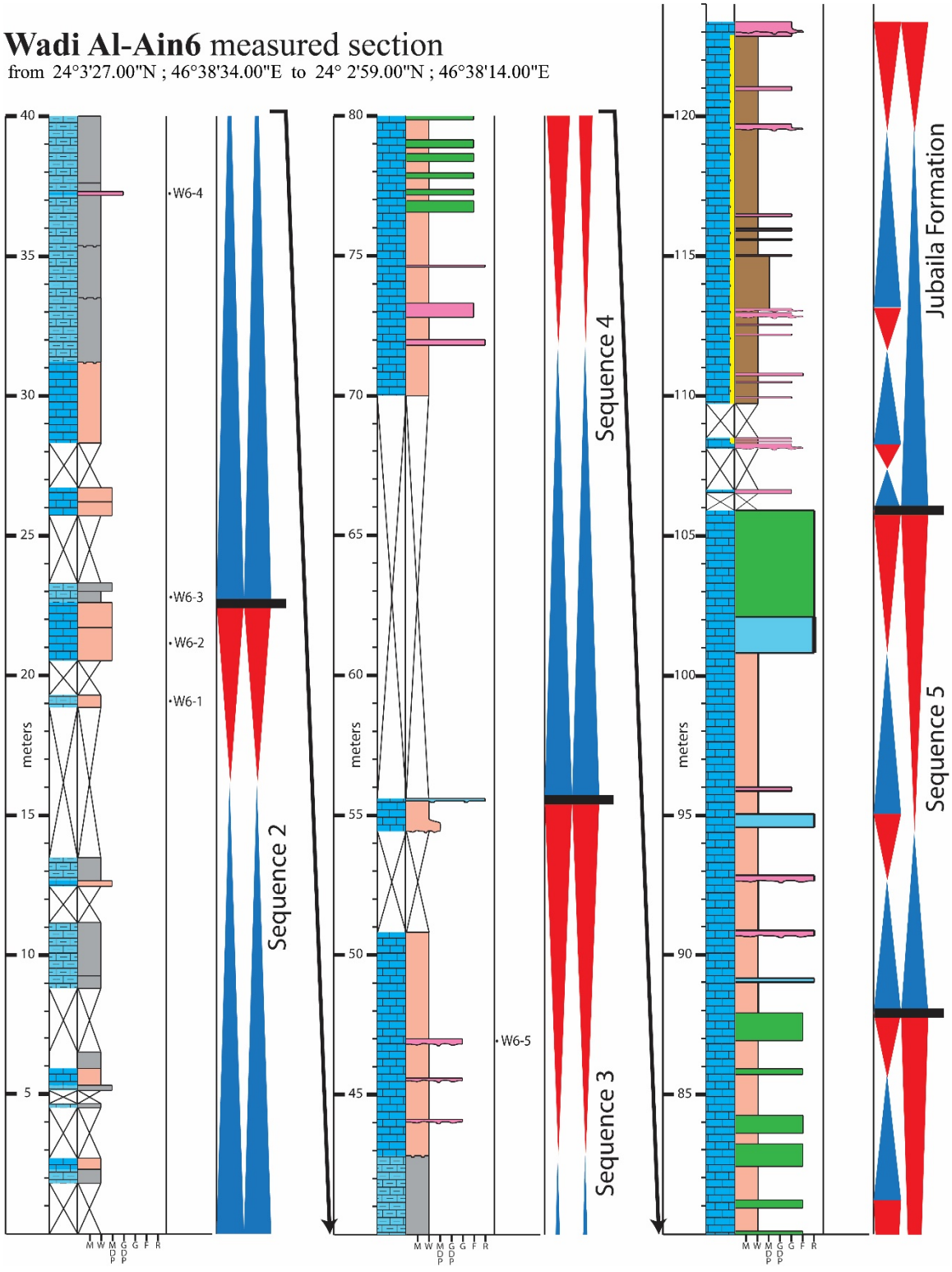
Wadi Al-Ain6 measured section
from 24°3'27.00"N ; 46°38'34.00"E to 24° 2'59.00"N ; 46°38'14.00"E
meters
W6-4
W6-3
W6-2
W6-1
W6-5
Sequence 2
Sequence 3
Sequence 4
Sequence 5
Jubaila Formation

REFERENCES

Aigner, T., 1982. Calcareous tempestites: storm-dominated stratification in Upper Muschelkalk Limestones (Middle Trias, SW-Germany), in: Einsele, G., Seilacher, A. (Eds.), Cyclic and Event Stratification. Springer-Verlag, New York, USA, pp. 180–198.

Aigner, T., 1985. Storm depositional systems: dynamic stratigraphy in modern and ancient shallow-marine sequences, Lecture Notes in Earth Sciences 3. Springer-Verlag, New York, USA.

Alsharhan, A.S., Magara, K., 1994. The Jurassic of the Arabian Gulf Basin: facies, depositional setting and hydrocarbon habitat. Canadian Society of Petroleum Geologists, Memoir 17, 397–412.

Bádenas, B., Aurell, M., 2001. Proximal-distal facies relationships and sedimentary processes in a storm dominated carbonate ramp (Kimmeridgian, northwest of the Iberian Ranges, Spain. Sedimentary Geology 139, 319–340.

Bosscher, H., Schlager, W., 1993. Accumulation Rates of Carbonate Platforms. The Journal of Geology 101, 345–355.

Bramkamp, R.A., Steineke, M., 1952. Stratigraphical introduction, in: Arkell, W.J. (Ed.), Jurassic Ammonites from Jebel Tuwaiq, Central Arabia. Philosophical Transactions of the Royal Society of London, Series B: Biological Sciences, pp. 241–314.

Brannan, J., Sahota, G., Gerdes, K.D., Berry, J.A.L., 1999. Geological evolution of the central Marib-Shabwa Basin, Yemen. GeoArabia 4, 9–34.

Droste, H., 1990. Depositional cycles and source rock development in an epeiric intra-platform basin: the Hanifa Formation of the Arabian peninsula. Sedimentary Geology 69, 281–296.

Campbell, C. V., 1967. Lamina, laminaset, bed and bedset. Sedimentology 8, 7–26.

Carlucci, J.R., Westrop, S.R., Brett, C.E., Burkhalter, R., 2014. Facies architecture and sequence stratigraphy of the Ordovician Bromide Formation (Oklahoma): a new perspective on a mixed carbonate-siliciclastic ramp. Facies 60, 987–1012.

Clifton, H.E., 2006. A reexamination of facies models for clastic shorelines, in: Posamentier, H.W., Walker, R.G. (Eds.), Facies Models Revisited. SEPM Special Publication 84, Tulsa, USA, pp. 293–337.

Colombié, C., Bádenas, B., Aurell, M., Götz, A.E., Bertholon, S., Boussaha, M., 2014. Feature and duration of metre-scale sequences in a storm-dominated carbonate ramp setting (Kimmeridgian, northeastern Spain). Sedimentary Geology 312, 94–108.

Colombié, C., Rameil, N., 2007. Tethyan-to-boreal correlation in the Kimmeridgian using high-resolution sequence stratigraphy (Vocontian Basin, Swiss Jura, Boulonnais, Dorset). International Journal of Earth Sciences 96, 567–591.

Dumas, S., Arnott, R.W.C., 2006. Origin of hummocky and swaley cross-stratification - The controlling influence of unidirectional current strength and aggradation rate. Geology 34, 1073–1076.

Dunham, R.J., 1962. Classification of Carbonate Rocks According to Depositional Texture, in: Ham, W.E. (Ed.), Classification of Carbonate Rocks - A Symposium.

AAPG Memoir 1, pp. 108–121.
El-Asa'ad, G.M.A., 1991. Oxfordian hermatypic corals from Central Saudi Arabia. Geobios 24, 267–287.
El-Asmar, H.M., Assal, E.M., El-Sorogy, A.S., Youssef, M., 2015. Facies analysis and depositional environments of the Upper Jurassic Jubaila Formation, Central Saudi Arabia. Journal of African Earth Sciences 110, 34–51. doi:10.1016/j.jafrearsci.2015.06.001
El-Sorogy, A.S., Al-Kahtany, K.M., 2015. Contribution to the scleractinian corals of Hanifa Formation, Upper Jurassic, Jabal Al-Abakkayn, central Saudi Arabia. Historical Biology 27, 90–102.
Embry, A.F., Klovan, J.E., 1971. A Late Devonian reef tract on northeastern Banks Island, N.W.T. Bulletin of Canadian Petroleum Geology 19, 730–781.
Enay, R., Le Nindre, Y.-M., Mangold, C., Manivit, J., Vaslet, D., 1987. Le Jurassique D'Arabie Saoudite Centrale: Nouvelles données sur la lithostratigraphie, les paléoenvironnements, les faunes d'ammonites, les âges et les corrélations, in: Enay, R. (Ed.), Le Jurassique D'Arabie Saoudite Centrale. Geobios Mémoire Spécial 9, pp. 13–65.
Fischer, J., Le Nindre, Y.-M., Manivit, J., Vaslet, D., 2001. Jurassic gastropod faunas of Central Arabia. GeoArabia 6, 63-100.
Flügel, E., 2010. Microfacies of carbonate rocks: analysis, interpretation and application, 2nd ed. Springer, New York, USA.
Friebe, J.G., 1993. Sequence stratigraphy in a mixed carbonate-siliciclastic depositional system (Middle Miocene; Styrian Basin, Austria). Geologische Rundschau 82, 281–294.
Fürsich, F.T., 1998. Environmental distribution of trace fossils in the Jurassic of Kachchh (Western India). Facies 39, 243–272.
Gradstein, F.M., Ogg, J.G., Schmitz, M.D., Ogg, G.M., 2012. The Geologic Time Scale 2012. Elsevier, New York, USA.
Haq, B.U., Hardenbol, J., Vail, P.R., 1988. Mesozoic and Cenozoic chronostratigraphy and cycles of sea-level change, in: Wilgus, C.K., Hastings, B.S., Kendall, C.G.St.C., Posamentier, H.W., Ross, C.A., Van Wagoner, J.C. (Eds), Sea-level changes: an integrated approach. SEPM Special Publication 42, Tulsa, USA, pp. 71-108.
Hughes, G.W., 2004. Middle to Upper Jurassic Saudi Arabian carbonate petroleum reservoirs: Biostratigraphy, micropaleontology, and paleoenvironments. GeoArabia 9, 79–114.
Hughes, G.W., Varol, O., Al-Khalid, M., 2008. Late Oxfordian micropalaeontology, nannopalaeontology and palaeoenvironments of Saudi Arabia. GeoArabia 13, 15–46.
Hughes, G.W., 2009. Using Jurassic micropaleontology to determine Saudi Arabian carbonate paleoenvironments. SEPM Special Publication No. 93, 127–152.
James, N., Jones, B., 2015. Origin of carbonate sedimentary rocks, 1st ed. Wiley, Hoboken, USA.
Jank, M., Wetzel, A., Meyer, C.A., 2006. Late Jurassic sea-level fluctuations in NW

Switzerland (Late Oxfordian to Late Kimmeridgian): Closing the gap between the Boreal and Tethyan realm in Western Europe. Facies 52, 487–519.
Kästner, M., Schülke, I., Winsemann, J., 2008. Facies architecture of a Late Jurassic carbonate ramp: the Korallenoolith of the Lower Saxony Basin. International Journal of Earth Sciences 97, 991–1011.
Kerans, C., Tinker, S.W., 1997. Sequence stratigraphy and characterisation of carbonate reservoirs, SEPM Short Course No. 40. Society for Sedimentary Geology, Tulsa, USA.
Knaust, D., 1998. Trace fossils and ichnofabrics on the Lower Muschelkalk carbonate ramp (Triassic) of Germany: tool for high-resolution sequence stratigraphy. Geologische Rundschau 87, 21–31.
Knaust, D., Curran, H.A., Dronov, A. V., 2012. Shallow-marine carbonates, in: Knaust, D., Bromley, R.G. (Eds.), Trace Fossils as Indicators of Sedimentary Environments. Developments in Sedimentology 64, Elsevier, Boston, USA, pp. 705–750.
Krause Jr., R.A., Meyer, D.L., 2004. Sequence stratigraphy and depositional dynamics of carbonate buildups and associated facies from the Lower Mississippian Fort Payne Formation of southern Kentucky, U.S.A. Journal of Sedimentary Research 74, 831–844.
Le Nindre, Y.-M., Manivit, J. H., Vaslet, D., 1990. Stratigraphie séquentielle du Jurassique et du Crétacé en Arabie Saoudite. Bulletin Societé Géologique France 8, 1025-1034.
Le Nindre, Y.-M., Vaslet, D., Le Métour, J., Bertrand, J., Halawani, M., 2003. Subsidence modeling of the Arabian Platform from Permian to Paleogene outcrops. Sedimentary Geology 156, 263–285.
Lindsay, R.F., Cantrell, D.L., Hughes, G.W., Keith, T.H., Mueller III, H.W., Russell, S.D., 2006. Ghawar Arab-D reservoir: widespread porosity in shoaling-upward carbonate cycles, Saudi Arabia, in: Harris, P.M., Weber, L.J. (Eds.), Giant Hydrocarbon Reservoirs of The World: From Rocks to Reservoir Characterization and Modeling. AAPG Memoir 88/ SEPM Special Publication, pp. 97–137.
Manivit, J., Pellaton, C., Vaslet, D., Le Nindre, Y.-M., Brosse, J.-M., Breton, J.-P., Fourniguet, J., 1985. Explanatory notes to the geologic map of the Darma' Quadrangle, sheet 24 H, Kingdom of Saudi Arabia, Saudi Arabian Deputy Ministry for Mineral Resources, Jeddah, Geosciences Map, GM-101C.
Markello, J.R., Koepnick, R.B., Waite, L.E., Collins, J.F., 2007. The carbonate analogs through time (CATT) hypothesis and the global atlas of carbonate fields—a systematic and predictive look at Phanerozoic carbonate systems. SEPM Special Publication No. 89, 1–31.
McGuire, M.D., Koepnick, R.B., Markello, J.R., Stockton, M.L., Waite, L.E., Kompanik, G.S., Al-Shammery, M.J., Al-Amoudi, M.O., 1993. Importance of sequence stratigraphic concepts in development of reservoir architecture in Upper Jurassic grainstones, Hadriya and Hanifa Reservoirs, Saudi Arabia, in: Proceedings of the 8th Society of Petroleum Engineers Middle East Oil Show, SPE Paper 25578. Richardson, TX, USA, pp. 489–499.

Molina, J.M., Ruiz-Ortiz, P.A., Vera, J.A., 1997. Calcareous tempestites in pelagic facies (Jurassic, Betic Cordilleras, Southern Spain). Sedimentary Geology 109, 95–109.
Moshrif, M.A., 1984. Sequential development of Hanifa Formation (Upper Jurassic) paleoenvironments and paleogeography, Central Saudi Arabia. Journal of Petroleum Geology 7, 451–460.
Nichols, G., 2009. Sedimentology and Stratigraphy, 2nd ed. Wiley-Blackwell, Hoboken, USA.
Okla, S.M., 1983. Microfacies of Hanifa Formation (Upper Jurassic) in Central Tuwaiq Mountains. Journal of College of Science, King Saud University 14, 121–143.
Okla, S.M., 1986. Litho- and microfacies of Upper Jurassic carbonate rocks outcropping in Central Saudi Arabia. Journal of Petroleum Geology 9, 195–206.
Olivier, N., Cariou, E., Hantzpergue, P., 2015. Evolution of a Late Oxfordian: early Kimmeridgian carbonate platform, French Jura Mountains. Swiss Journal of Geosciences 108, 273–288.
Olivier, N., Colombié, C., Pittet, B., Lathuilière, B., 2011. Microbial carbonates and corals on the marginal French Jura platform (Late Oxfordian, Molinges section). Facies 57, 469–492.
Powers, R.W., Ramirez, L.F., Redmond, C.D., Elberg, E.L.J., 1966. Geology of the Arabian Peninsula: sedimentary geology of Saudi Arabia. U.S. Geological Survey Professional Paper 560–D, 154.
Powers, R.W., 1968. Saudi Arabia (excluding the Arabian Shield). Lexique Stratigraphique International III.
Scholle, P.A., Ulmer-Scholle, D.S., 2003. A color guide to the petrography of carbonate rocks: grains, textures, porosity, diagenesis. AAPG Memoir 77, Tulsa, USA.
Scotese, C.R., 2002. PALEOMAP website. URL http://www.scotese.com, Last accessed on 19 March, 2017.
Seguret, M., Moussine-Pouchkine, A., Gabaglia, G.R., Bouchette, F., 2001. Storm deposits and storm-generated coarse carbonate breccias on a pelagic outer shelf (South-East Basin, France). Sedimentology 48, 231–254.
Sharland, P.R., Archer, R., Casey, D.M., Davies, R.B., Hall, S.H., Heward, A.P., Horbury, A.D., Simmons, M.D., 2001. Arabian Plate Sequence Stratigraphy. GeoArabia Special Publication 2, Manama, Bahrain.
Taylor, A.M., Goldring, R., 1993. Description and analysis of bioturbation and ichnofabric. Journal of the Geological Society, London 150, 141–148.
Vaslet, D., Al-Muallem, M.S., Maddah, S.S., Brosse, J.-M., Fourniguet, J., Breton, J.-P., Le Nindre, Y.-M., 1991. Explanatory Notes to the Geologic Map of the Ar Riyad Quadrangle, Sheet 24 I, Kingdom of Saudi Arabia, Saudi Arabian Deputy Ministry for Mineral Resources, Jeddah, Geosciences Map, GM-121C. Jeddah, USA.
Vaslet, D., Manivit, J., Le Nindre, Y.-M., Brosse, J.-M., Fourniguet, J., Delfour, J., 1983. Explanatory Notes to the Geologic Map of the Wadi Ar Rayan Quadrangle, Sheet 23 H, Kingdom of Saudi Arabia, Saudi Arabian Deputy Ministry for Mineral Resources, Jeddah, Geosciences Map, GM-63A. Jeddah, KSA.
Védrine, S., Strasser, A., Hug, W., 2007. Oncoid growth and distribution controlled by

sea-level fluctuations and climate (Late Oxfordian, Swiss Jura Mountains). Facies 53, 535–552.
Ziegler, M.A., 2001. Late Permian to Holocene paleofacies evolution of the Arabian Plate and its hydrocarbon occurrences. GeoArabia 6, 445–504.